A Fluorescence In Situ Hybridization Approach for Gene Mapping and the Study of Nuclear Organization

Jeanne Bentley Lawrence

Department of Cell Biology
University of Massachusetts Medical School
Worcester, Massachusetts 01655

In situ hybridization procedures that directly couple molecular and cytological information have very recently had a surge of success in powerful new applications. Pivotal to these advances has been technological improvements that allow the precise visualization of single sequences within individual metaphase and interphase cells. This has important implications for human gene mapping and clinical cytogenetics. These techniques provide not only an important tool for determining linear arrangements of genes on individual chromosomes, but also a powerful approach for analysis of their three-dimensional organization and expression within the genome. Hence, the ability to detect individual genes, viral genomes, or primary nuclear transcripts sensitively has significance for cell and developmental biology as well.

This chapter discusses:

- ❑ the current state of the art and the potential of high-sensitivity fluorescence in situ hybridization methodology
- ❑ recent contributions to this field from our laboratory
- ❑ applications for human genome mapping and for investigating higher-level genome organization
- ❑ a new approach, termed interphase chromatin mapping, that allows the rapid precise localization of closely spaced DNA sequences along the chromatin fiber
- ❑ potential applications for analysis of cytogenetic aberrations

Genome Analysis Volume 1: Genetic and Physical Mapping

INTRODUCTION

Many laboratories have contributed to the development and application of cytological hybridization, with advances being made in stages over a period of 20 years. This technology has progressed from a laborious and time-consuming approach to detect abundant nucleic acid sequences with low resolution to an approach that allows fast, highly precise, and sensitive localization of as little as one molecule per cell. Although it is not possible to review all of the work in this field, this section attempts to summarize briefly the major contributions leading to the current state of the art, before describing work from our laboratory.

The concept of applying molecular hybridization directly to cytological material was initially pioneered by Gall and Pardue (1969) and John et al. (1969). The early phase of the development of this field relied on autoradiographic detection of radioactive probes to localize abundant sequences, such as localization of DNA sequences in amplified polytene chromosomes and highly reiterated sequences on metaphase chromosomes (Evans et al. 1974). During the following decade, applications were generally restricted to highly represented sequences. In 1981, two reports (Gerhard et al. 1981; Harper et al. 1981) showed that it was possible to localize single sequences on metaphase chromosomes by autoradiography of ^{125}I- or ^{3}H-labeled probes. This approach has since been used to map many genes and is the most frequently used in-situ-mapping method to date. However, autoradiography has several significant limitations. Because of the scatter of radioactive disintegrations, the resolution is limited to relatively large chromosomal segments. Furthermore, localization of the sequence is not determined directly within a single cell but requires statistical analysis of grain distribution in as many as 50–100 metaphase figures. In addition, the technique is extremely time-consuming, since weeks are generally required for sufficient autoradiographic exposures. Although autoradiography offers the advantage that cDNA sequences of less than 1 kb can be used routinely for statistical localization, this approach is not used for genomic clones containing repetitive sequences, presumably because of prohibitively high backgrounds.

To overcome the limitations of autoradiography, several laboratories had the foresight to pursue development of innovative nonisotopic detection techniques. One of the earliest nonisotopic in situ detections used an antibody to RNA-DNA hybrids (Rudkin and Stollar 1977). In 1980, a method for direct labeling of fluorochromes to DNA probes was described (Bauman et al. 1980, 1981). Several indirect nonisotopic techniques were developed using chemically modified DNA probes, which are detected after hybridization by affinity reagents. The development of the avidin:biotin system was originated and developed initially using methacrylate spheres or ferritin detectors for electron microscopic

localization of tRNAs or rRNA (Manning et al. 1975; Broker et al. 1978). Subsequently, the incorporation of biotinylated dUTP into a DNA probe (Langer et al. 1981) and detection by a two-step antibiotin antibody reaction after hybridization to amplified sequences in polytene chromosomes were described (Langer-Safer et al. 1982). Probes labeled with AAF (*N*-acetoxy-*N*-acetyl-2-aminofluorene), for which antibodies were readily available, were subsequently reported and successfully applied for detection of abundant sequences (Tchen et al. 1984). In efforts to produce more sensitive or convenient technology, several groups continued to develop alternative labeling techniques, such as mercuration of probes (Dale et al. 1975; Hopman et al. 1986), sulfonation (Verdlov et al. 1974), and direct attachment of horseradish peroxidase (HRP) (Renz and Kurz 1984). Most recently, a very effective system has been described that uses digoxygenin-labeled nucleotides detected by antibodies carrying fluorescent or enzymatic tags (Boehringer Mannheim).

Fluorescent or enzymatic reporter molecules were most frequently used to detect probes labeled by various means. Commonly used enzymes have been HRP and alkaline phosphatase. The enzymatic detection methods require extra steps to convert the substrate to a visible product; however, they have an advantage over fluorescence in that the enzyme reaction can be prolonged in order to amplify signals and the signals do not fade. Fluorescent tags are advantageous in that they provide the highest resolution possible with the light microscope and are easily adapted for multicolor labeling and for quantitation and processing by a variety of instrumentations. Fluorescein isothiocyanate (FITC) and rhodamine isothiocyanate (TRITC) are the most frequently used, but other fluorochromes with different spectral properties are becoming more widely available. Efforts to improve the detection from fluorescent tags have been directed at amplification of the detector, such as by antibody-stacking techniques (Pinkel et al. 1986), and through the use of sensitive digital cameras and computerized image enhancement.

During the past decade, different nonisotopic labeling techniques using fluorescent or enzymatic reporters have been variously applied for detecting highly repeated DNA sequences or abundant mRNAs. For example, nonisotopic hybridization to satellite DNA was reported as early as 1982 (Manuelidis et al.), amplified sequences were localized in polytene chromosomes (Wu and Davidson 1981; Langer-Safer et al. 1982; Kress et al. 1985), and clustered genes for rRNAs were detected on metaphase chromosomes (van Prooijen-Knegt et al. 1982; Albertson 1985). Although nonisotopic detection became more widely applied for highly represented sequences, the detection of single-copy genes during this period was done almost exclusively by autoradiography. There were a few reports of some success in the nonisotopic detection of large (25–50 kb) unique sequences using specialized procedures to amplify signals from either AAF-labeled probes using interference reflection mi-

croscopy (Landegent et al. 1985) or biotin-labeled probes for mapping in *Caenorhabditis elegans* using image processing (Albertson 1985). These procedures were not widely adopted over radioactive techniques, largely because of limitations of sensitivity and reproducibility in a growing number of nonisotopic methods. Recently, the overall performance of the technology in terms of a combination of hybridization efficiency, signal-to-noise ratios, sensitivity, and resolution was sufficiently enhanced to allow fluorescence in situ hybridization to emerge as an invaluable tool with far-reaching applications in genetic, cell biological, virological, and clinical investigations.

The difficulty of applying these techniques for single-sequence detection had been generally considered a consequence of limitations in detection sensitivity. However, the most recent advances in the success of this technology use innovative detection techniques described several years earlier and derive primarily from improvements in hybridization conditions and other parameters of the total process. Our laboratory's contribution has not been in the development of detection techniques but in analytical investigation of the most successful conditions for high-efficiency cytological hybridization with nonisotopic probes.

QUANTITATIVE ANALYSIS OF HYBRIDIZATION PARAMETERS

Conceptually and technically, the process of hybridization and detection of specific nucleic acids within cytological material is complicated relative to the straightforward situation in which isolated nucleic acids stripped of protein are bound to a uniform substance, such as a nitrocellulose filter. For analytical purposes, the steps of in situ hybridization can be divided into three main components, each of which is essential for success:

1. *Preservation.* Target sequences must be well-preserved throughout hybridization but remain in an accessible state within the biological material. Although this is especially critical for RNA, it is an important consideration for detection of nuclear or chromosomal DNA as well.
2. *Hybridization.* The probe must hybridize the target molecules with high efficiency without substantial nonspecific adherence to biological material, which is inherently reactive.
3. *Detection.* The reporter must bind to the probe in sufficient quantities to give a detectable signal, while sources of nonspecific background from the detector or the cellular material itself are minimized.

Failure of any one parameter in any of these components results in a lower signal-to-noise ratio and a loss of sensitivity for a given detection system. The potential of nonisotopic probe technology could not be fully realized until important parameters were identified, optimized, and put together in the appropriate combination to push the practical capabilities of this technology closer to its theoretical potential. To this end, we emphasized quantitative characterization of hybridization and detection parameters to provide higher hybridization efficiency. The goal for single-copy genes was to obtain hybridization efficiencies high enough to provide sister-chromatid labeling and nonstatistical localization. Microscopy was generally too laborious and subject to internal variation to allow a very thorough analysis of numerous hybridization parameters and their various combinations. An analytical approach was implemented that allowed rapid quantitation of numerous parameters and allowed the success of the preservation, hybridization, and detection components to be evaluated separately. This was initially done for detecting cytoplasmic mRNAs and later extended to nuclear DNA (Lawrence and Singer 1985; Singer et al. 1986, 1987; Lawrence et al. 1988). A number of nonobvious parameters were sorted out and unexpectedly found to be important.

Some of the key parameters identified for single-sequence detection by this quantitative approach are illustrated below, and other technical details can be found in previously published reports (see Lawrence et al. 1988, 1989, 1990a) and in the brief protocol provided at the end of the chapter.

Reducing avidin background for detection of biotinylated probes

We initially used ^{125}I-labeled avidin to assess a means of reducing the widely reported nonspecific adherence of this protein to cytological material, as summarized in Table 1 (Singer et al. 1987). The main conclusion of this work was that the presence of phosphate-buffered saline (PBS), which had been generally used previously (Langer-Safer et al. 1982; Singer and Ward 1982), promoted high nonspecific sticking of avidin. This was to some extent surprising because avidin diluted in PBS was routinely used with success to detect biotinylated probes on filters. The nonspecific sticking of avidin can be reduced by approximately 90% using sodium citrate, preferably of higher salt concentration (4× SSC). Neither acetic anhydride, nor detergents, nor changes in pH reduced the avidin background. The various chemically modified forms of avidin, developed commercially to reduce its background, are unnecessary for this purpose and in some cases give less-intense signals than fluorescein-avidin.

Table 1 ^{125}I-labeled avidin bound to cells with various treatments (average of duplicate samples)

Treatment	Counts per minute
No cells (glass coverslip; 1× SSC)	139
With cells (1× SSC)	1,348
Acetic-anhydride-treated cells (1× SSC)	1,365
Triton-treated cells (1× SSC)	1,905
Cells in PBS	16,406
Cells in PBS with 100 µg/ml cold avidin	1,288
Cells in PBS with 1 mg/ml cold avidin	928
Cells in 4× SSC (pH 5.2)	1,174
Cells in 4× SSC (pH 6.2)	844
Cells in 4× SSC (pH 7.2)	1,235
Cells in 4× SSC (pH 8.2)	747

Data from Singer et al. (1987).

Hybridization kinetics

Further analysis demonstrated that the fluorescein-avidin detection, when applied under appropriate conditions, was extremely sensitive but that the hybridization component was failing (Fig. 1A).

Figure 1 (*A*) An early attempt at fluorescence detection of hybridization to single-copy genes, illustrating a common result of hybridization with low probe concentrations (no specific signal) and large probe fragment size (high spotty background). This experiment used probes labeled with both ^{32}P and biotin and showed that the detection component was working with sensitivity, but that the hybridization component was failing. The hybridization conditions led to high background and no specific signal. (*B*) Total human genomic DNA or *Escherichia coli* DNA was nick-translated with ^{32}P dCTP and hybridized to samples of HeLa cell chromosome preparations, and the results were quantitated by scintillation. *Effect of time:* (*Open squares*) Human DNA probe; (*closed squares*) *E. coli* control probe to assess background. Hybridization was carried out for the times indicated at 37°C at a constant concentration of 4 ng/10 µl/sample. Each point represents the average of triplicate samples. *Effect of concentration:* The probe concentration is expressed as the nanograms of probe applied per sample in 10 µl of volume. (*Open circles*) Human DNA probe; (*closed circles*) *E. coli* control probe to assess background. Hybridization was carried out at 37°C for 16 hr, and each point represents the average of duplicate samples. (Reprinted, with permission, from Lawrence et al. 1988.) (*C*) Fluorescence detection of sequences within interphase nuclei. The EBV *Bam*HI W probe was hybridized to Namalwa cell nuclei. Note that two viral genomes are visible in the smaller G_1 nucleus (*right*), whereas four signals are observed in the larger tetraploid or G_2 nucleus. (Reprinted, with permission, from Lawrence et al. 1988.) (*D*) Two probes (*Bam*HI W and A), separated by 130 kb within the EBV genome, were hybridized simultaneously to Namalwa cell nuclei. The presence of four tightly clustered spots of two different intensities (due to two different-size target sequences) is observed in many G_1 nuclei. (Reprinted, with permission, from Lawrence et al. 1988.) (*E*) Diagram illustrating the interpretation of the pattern shown in *D* and described in the text.

A similar quantitative approach was applied for optimizing hybridization to chromosomal and nuclear DNAs. To generate sufficient signal for rapid quantitation of many samples, we used total human DNA labeled with ^{32}P as a probe for hybridization to standard preparations of chromosomes. Numerous technical parameters were tested, and two are presented here to illustrate the approach.

The efficiency of hybridization to single-copy sequences was generally low as analyzed by autoradiographic techniques, and standard protocols called for long hybridization times (1–4 days) and low concentrations of probe (<1 ng per sample) (Gerhard et al. 1981; Harper et al. 1981; Harper and Marselle 1985). In Figure 1B, the kinetics of the in situ hybridization process were evaluated on the basis of triplicate samples in replicate experiments. The striking feature of these results was that hybridization rose very sharply, with the reaction being one-third maximal in just 10 minutes and essentially complete within 4 hours. In some experiments, a slight decrease in signal occurred with prolonged incubations, probably because of dissolution of the sample. Since hybridization of low-copy sequences should continue to occur over a longer period of time, these results first indicated that the rapid reannealment of chromosomal DNA may limit hybridization efficiency and

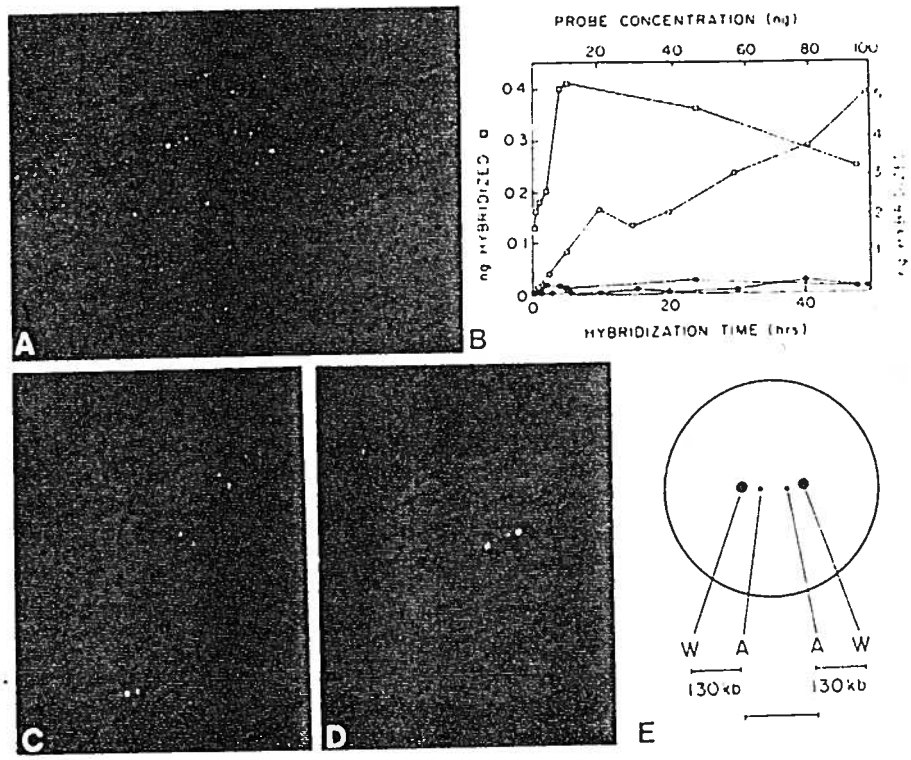

Figure 1 (*See facing page for legend.*)

should be competed with extremely high probe concentrations, rather than prolonged hybridization times and low probe concentrations.

These conclusions led us to evaluate the effect of probe concentration on signal and noise, since high probe concentrations are generally considered prohibitive because of increased background. Repeated experiments yielded similar results, as illustrated in Figure 1B. Note that hybridization was still rising rapidly at 200 ng per coverslip (10 µg/ml or over 100 times more DNA than was used routinely in hybridizations), whereas background increased only very gradually. Hence, at high probe concentrations, the extent of hybridization is much greater, although the signal-to-noise ratio can be as good as or better than that at low concentrations, since hybridization rises more sharply than background. These results suggested that better hybridization efficiencies could be obtained by changing in situ hybridization strategies to relatively short hybridization times and high probe concentrations, which would ordinarily be expected to be well above saturation. However, in other experiments, it was determined that high concentrations of nonisotopic probes, such as biotinylated probes, could only be used successfully if another key parameter, the probe fragment size, was carefully controlled.

Probe fragment size

For filter hybridization, it is reasonably assumed that two labeled preparations of the same probe that have equivalent specific activities will yield comparable results. This is emphatically not the case for in situ hybridization because the fragment size after labeling (commonly by nick translation) impacts on:

1. The penetration of the probe into the cytological material. This factor has been considered previously by several groups and is particularly important for tissue sections and intact cells.
2. The nonspecific adherence of the probe to cytological material (Lawrence and Singer 1985; Singer et al. 1986; Lawrence et al. 1990a). This is an extremely important parameter for in situ hybridization, especially with nonisotopic probes. Probe sticking has been a very common source of failure in the past.
3. The networking of the probe to amplify signals (Lawrence and Singer 1985).
4. The iterative detection of individual molecules (i.e., if several probe fragments hybridize to a single target sequence, the signal will be distributed differently than the noise). This is most clearly observed for electron microscopy detection (Singer et al. 1989), but it is also a significant factor in generating high signal-to-noise ratios with fluorescence.

Other technical variables

Other parameters found to influence the quality of the results were the frozen storage of slides and their "hardening" by baking before denaturation; minimizing pretreatments prior to denaturation; omitting RNase A digestion prior to hybridization (which is generally unnecessary but can be replaced by RNase H after hybridization); testing of lots of formamide for neutral pH, correct melting point, and effectiveness for hybridization; careful monitoring of time, temperature, and pH during the denaturation step; and autoclaving the dextran sulfate, which chemically modifies it in such a way that it causes less nonspecific sticking of probes at high concentrations. In addition, a variety of other steps that existed in the literature were tested and found to be unnecessary. For example, extensive rinsing of the samples made no difference in the results, and proteinase digestion was generally found to be unnecessary. Acetic anhydride, useful for some cell types with high endogenous backgrounds, is not necessary for chromosomal hybridizations.

HIGH-EFFICIENCY FLUORESCENCE HYBRIDIZATION

We emphasized fluorescence, as did other investigators, because it is the simplest yet highest-resolution detection and because initial attempts indicated that it could be quite sensitive provided hybridization were improved (Fig. 1A). With attention to the variables identified above, we demonstrated that a one-step fluorescein-avidin detection, without amplification or image-processing procedures, could detect single sequences as small as 5 kb by standard fluorescence microscopy (Lawrence et al. 1988). Although first done with biotinylated probes, the same conditions can be used to detect smaller sequences of a few kilobases or less using digoxygenin-labeled probes, for instance, to detect single copies of the human immunodeficiency virus (HIV) genome (Lawrence et al. 1990b). This work showed that it was possible to obtain extremely high hybridization efficiency and low backgrounds, such that bona fide hybridization to fragments of an integrated Epstein-Barr virus (EBV) genome could be confidently identified in greater than 90% of individual metaphase or interphase cells. Identical sister-chromatid labeling, coupled with negligible background (see Fig. 9A), allowed unequivocal localization within a single cell, qualitatively distinct from autoradiographic or enzymatic procedures that were statistical in nature. In addition to applications for chromosome mapping, this work showed it was possible to detect and localize single sequences within interphase nuclei precisely, which had implications for both gene mapping and the study of nuclear organization.

The demonstration that very tightly linked DNA sequences within decondensed interphase nuclei could be resolved by light microscopy

(Lawrence et al. 1988) was an initially surprising outcome of this work and revealed that genes must be farther apart than would be predicted by the total condensation of nuclear DNA, known to be 1:1000 or greater (Lewin 1985). In the Namalwa cell line studied, the EBV genome was integrated on only one chromosome-1 homolog, yet paired fluorescent signals separated by 0.2–3 μm were observed in the vast majority of interphase nuclei. Further analysis provided evidence that the two spots represented two copies of the EBV genome incorporated at a single chromosomal site, which became apparent in the less-condensed interphase nucleus (Fig. 1C). The observation that larger nuclei, either in G_2 phase or tetraploid, frequently had two "pairs" of spots (Fig. 1C) was further consistent with this interpretation. Close examination of metaphase chromosomes, in which the DNA is more condensed and the two signals may coalesce, showed that the signal on each sister chromatid consists of a doublet of two very closely spaced fluorescent spots (up to 0.4 μm apart). Hence, the G_2 content of the metaphase cell also produced two pairs of spots. These results, indicating the presence of two viral genomes, coupled with evidence for only one set of virus-cell junction sequences (Matsuo et al. 1984) suggested that a duplication of viral and adjacent cellular sequences occurred during or after integration.

To verify this interpretation and to test further the resolving power of the technology, experiments were conducted to determine whether sequences at opposite ends of a single EBV genome could be simultaneously and individually visualized at interphase. In many nuclei, hybridization to the A fragment of each viral genome could be visually resolved from hybridization to the corresponding W fragment, separated by only 130 kb. Four tightly clustered spots were discernible in many interphase nuclei, two of which were dimmer and two of which were brighter, as shown in Figure 1D. Because the smaller A fragment (12 kb) consistently showed a dimmer signal than the larger W fragment (30 kb), it was surmised that the two dimmer spots represented A and the brighter spots represented W. The four uniformly bright spots observed in larger G_2 or tetraploid nuclei hybridized with just the W probe (Fig. 1C) were qualitatively different from the clustered spots of two different intensities observed in smaller (presumably G_1) nuclei hybridized simultaneously with A and W. Occasionally, the configuration of these four spots appeared in an extended linear array, as shown in Figure 1D, indicating that the orientation of the two integrated EBV genomes was W-A-A-W (Fig. 1E) and that roughly 220 kb of cellular DNA separated them.

These results were corroborated by a different approach. If the W-A-A-W orientation were correct, it would predict that the distance between signals with the W probe alone would be greater than with the A probe alone. Separate hybridizations were conducted, and the average distances between paired signals were determined in 125–150 randomly

selected nuclei. The average distance between A-A was consistently different from that between W-W in the predicted direction (0.99 ± 0.09 vs. 1.74 ± 0.14, respectively). This difference was highly significant statistically (p <0.001), confirming the above results which indicated that the EBV genome integrated as an inverted repeat in a W-A-A-W orientation. These data also provided an independent assessment of the distance between the two genomes as approximately 340 kb. The two estimates of this distance (220 kb and 340 kb) derived by two different approaches were relatively close, given the expected difficulty of approximating molecular distances on the basis of in situ hybridization.

These results led us to propose an approach to gene mapping, termed interphase chromatin mapping (Lawrence et al. 1988), whereby the physical proximity of tightly linked DNA sequences could be directly evaluated by hybridization to interphase nuclei. Studies were then initiated aimed at exploring and further developing the potential of interphase and metaphase fluorescence hybridization for genome analysis, as described below.

APPLICABILITY FOR HUMAN GENE MAPPING

The Human Genome Project is in an early stage of an ongoing worldwide effort to produce a genomic map of markers having an initial resolution of 1–5 cM, upon which a much-higher-resolution map will be based. Figure 2 gives an overview of the range of DNA distance measurements approachable by established mapping techniques and compares these with fluorescent in situ techniques. Genetic recombination analysis is an essential method for localizing disease genes with a limit of resolution of approximately 1 cM (~1 Mb), but it can only be used for sequences containing a restriction-fragment-length polymorphism (Botstein et al. 1980). Sequences less than 1 Mb apart are approachable by the technique of pulsed-field gel electrophoresis (PFGE) (Schwartz and Cantor 1984; Cantor et al. 1988), provided specific restriction enzyme sites are appropriately distributed in the area of interest. Somatic cell hybridization (Ruddle 1973; Ruddle and Creagan 1975) and autoradiographic in situ hybridization (Gerhard et al. 1981; Harper et al. 1981) have proven invaluable for localizing sequences to specific chromosomes or chromosome segments, but these techniques generally provide less resolution, in the range of 10^4 to 10^5 kb. Although both genetic recombination and PFGE are enormously useful approaches, there is a strong need for alternative or complementary physical linkage mapping methods capable of resolving anonymous DNA sequences 1–2 Mb or less apart. It would be particularly valuable if such methodology could be applied across a broad range of genetic distances to help bridge what is

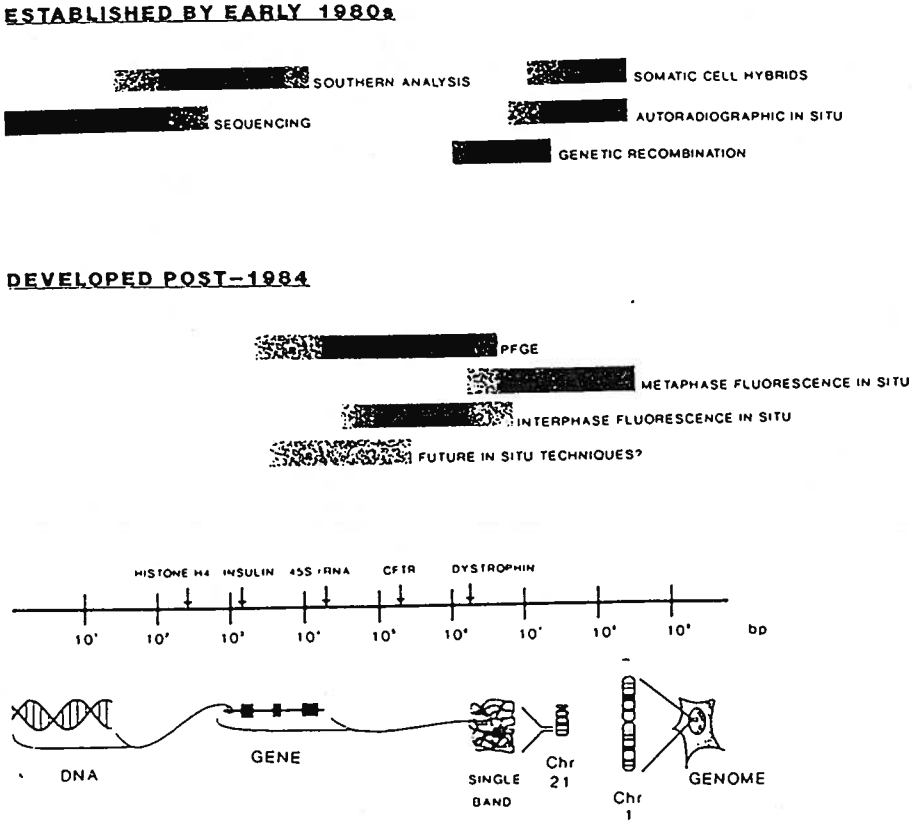

Figure 2 Comparison of the range of DNA distances over which different gene mapping techniques can be used. Lighter regions of each bar indicate a range for which the method has variable utility. Techniques are displayed from top to bottom in approximate chronological order. (*Gray bars*) Fluorescence in situ hybridization approaches; (*black bars*) other techniques. (PFGE) Pulsed-field gel electrophoresis; (CFTR) cystic fibrosis transmembrane regulator.

Figure 3 Hypothetical outcomes after hybridization of two single-copy probes to interphase and metaphase cells. Simultaneous hybridization of two probes to cytogenetic preparations containing both metaphase chromosomes and interphase nuclei is visualized by routine fluorescence microscopy. Unlinked or nonsyntenic sequences are readily resolved at both metaphase and interphase (*A*). Metaphase cells have a G_2 DNA content and hence twice as many signals as G_1 interphase cells because of the identical labeling of sister chromatids. Loosely linked sequences (*B*) will be resolvable along the chromosome length and show only a distant pairing within interphase nuclei. As sequences from the same chromosomal region become closer, they will no longer be resolvable along the chromosome length but may be separable across the width (*C*). Sequences difficult or impossible to resolve at metaphase will still be clearly visualized as closely paired signals within decondensed interphase nuclei (*D*), with the distance between paired signals proportional to DNA distance. The closest physical linkage (*E*) would be represented by sequences too close to resolve at either metaphase or interphase. The empirical support for these possible outcomes is provided in the following figures: Figure 4, outcome *A*; Figure 7A,B, outcome *B*; Figure 7C, outcome *C*; Figure 7D–H, outcome *D*; Figure 7I, outcome *E*.

often a difficult gap between information provided by lower- and higher-resolution techniques.

Results described above indicate the feasibility of coupling interphase and metaphase analyses to assess physical linkage across a broad range of distances, encompassing those approachable by autoradiographic in situ hybridization, genetic recombination, and PFGE. Figure 3 outlines a potential approach for rapidly evaluating the location and physical proximity of any two DNA segments. For clarity, a simple one-step detection scheme is described. Although not essential, multiple-label hybridization techniques with three or more probes can be incorporated to enhance the speed of information acquisition. In the outlined scheme, the respective locations of unlinked or loosely linked se-

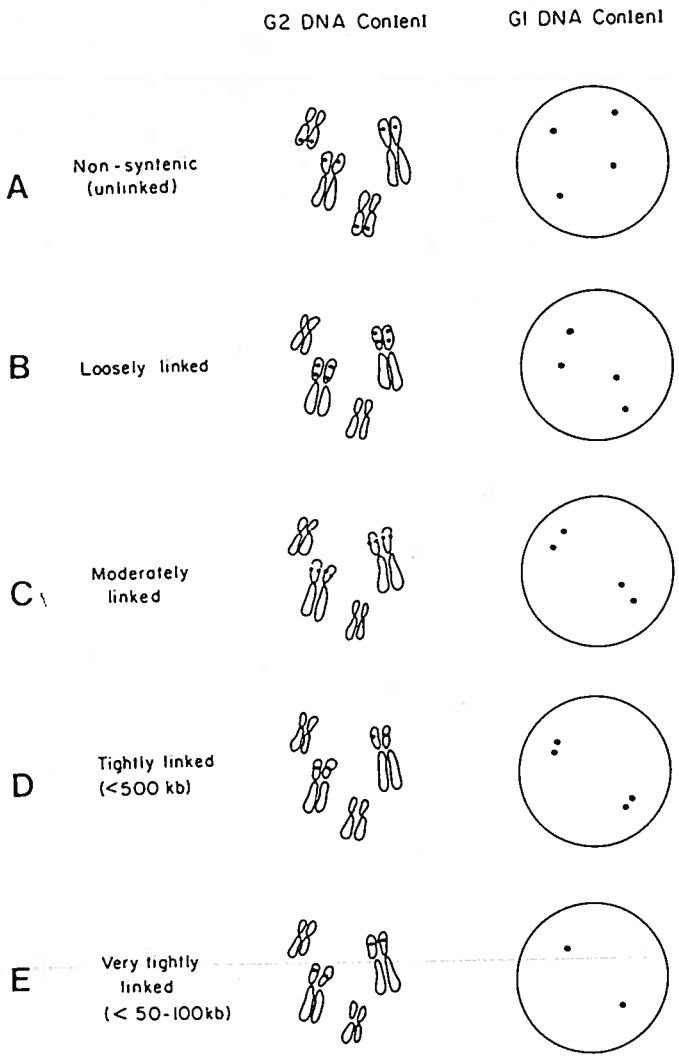

Figure 3 *(See facing page for legend.)*

quences are visualized on the metaphase chromosome. As sequences become too close to resolve at metaphase, they are still resolvable over a specific range in interphase chromatin, below which they coalesce into a single interphase signal, indicating very tight linkage. A distinction is made as to whether sequences are resolved along the length or the width of metaphase chromosomes, since the width of the chromosome is of sufficient dimension to encompass substantial lengths of DNA. The feasibility and limits of resolution for outcomes depicted in Figure 1 are characterized below.

Metaphase mapping

Detection of genomic probes containing repetitive elements It was important for the general applicability of this approach that genomic probes containing repetitive DNA be used, because direct fluorescence detection currently requires a few kilobases of target sequences. Competition of hybridization to repetitive sequences using total genomic DNA has been used routinely for filter hybridization, and for in situ detection of whole-chromosome libraries (Lichter et al. 1988; Pinkel et al. 1988). For single sequences, this was initially reported for cosmids detected with HRP and interference reflection microscopy using competition with Cot-1 human DNA (Landegent et al. 1987). This approach has been independently applied in a few laboratories for fluorescence detection, primarily for cosmids with >35-kb inserts (Trask et al. 1989; Lichter et al. 1990), and in our laboratory, it works routinely for phage probes with 10-kb inserts (Staunton et al. 1989; Lawrence et al. 1990). Figure 4 illustrates simultaneous localization of a phage probe and a cosmid probe using competition with unlabeled excess total human DNA and is representative of more than 90% of the phage or cosmid clones tested. Figure 4 also illustrates that a straightforward "double label" can be obtained using a single detection system by targeting different-size sequences. Identical labeling of sister chromatids allows rapid and definitive identification of two genes within one metaphase figure, in contrast with autoradiographic or enzymatic techniques with lower resolution that may more readily detect smaller sequences (Garson et al. 1987) but require statistical analysis of many metaphases to localize a single gene.

Comparison of different approaches An important and straightforward application of the ability to visualize hybridization within individual metaphases is that a sequence may be rapidly localized in terms of its relative position along the length of unbanded chromosomes. Lichter et al. (1990) localized 36 chromosome-11 cosmids using image processing to determine the ratio of signal position to total chromosome length. This work correctly ordered sequences comparable to results of somatic

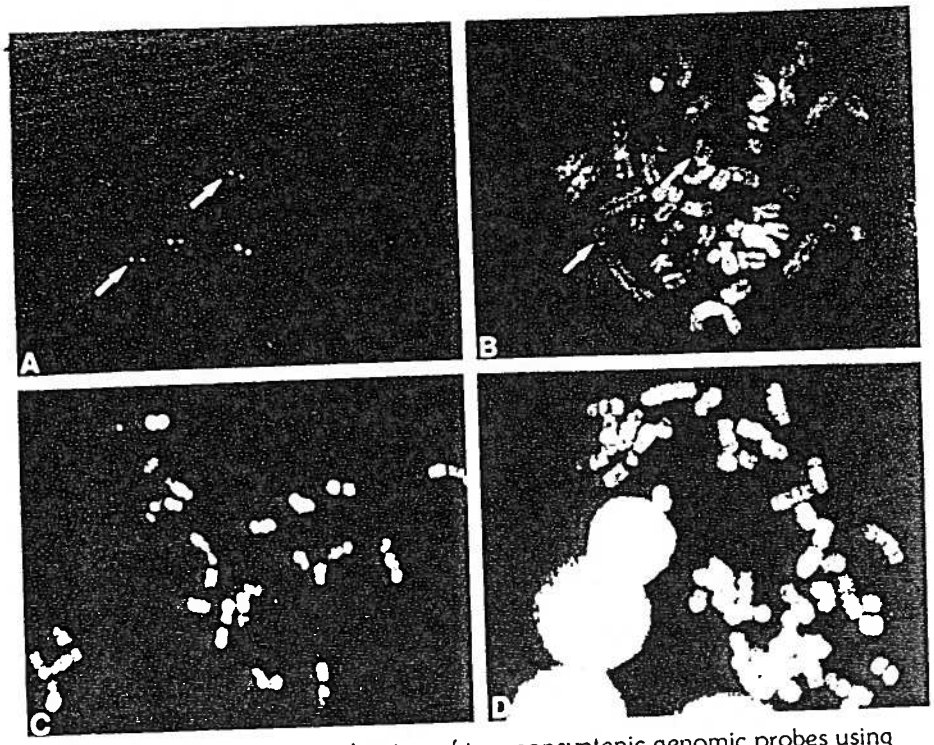

Figure 4 Simultaneous visualization of two nonsyntenic genomic probes using competition hybridization and intensity double-labeling. (*A*) Simultaneous hybridization to the *neu* proto-oncogene and α-cardiac myosin-heavy-chain (MHC) gene in the presence of 0.15 mg/ml of DNase-digested unlabeled total human placenta DNA. Repetitive hybridization (see *C,D*) is almost entirely eliminated, allowing the single-copy component of the targets to be detected. The phage and cosmid probes give different signal intensities because of the smaller (12 kb) target size of the MHC probe (*arrows*) compared with the *neu* cosmid (35 kb). (*B*) DAPI total DNA staining of chromosomes shown in *A*. Arrows indicate the positions of the dimmer MHC signals (see *A*). The α-cardiac MHC gene previously localized to chromosome 14 (Saez et al. 1987) can be regionally localized just beneath the centromere on the long arm of this chromosome, and the *neu* gene has been previously localized to chromosome 17. (*C,D*) Hybridization of each genomic probe separately in the absence of unlabeled excess human genomic DNA results in hybridization to repetitive DNA dispersed throughout the genome. The single-copy sequence is masked by the repetitive hybridization, which produces light and dark regions or "bands" on the chromosomes that vary depending on the particular repetitive elements present in the probe. Residual repetitive hybridization can be useful for visualizing chromosome morphology and aids in chromosome identification. (*C*) Cosmid probe for the *neu* proto-oncogene (*erbB2*) (White et al. 1987). (*D*) Phage probe for the α-cardiac MHC gene (Saez et al. 1987).

cell hybridization with deleted chromosomes. Because the entire cytogenetic map is currently expressed in terms of chromosome bands, it was important that this technique could be coupled with cytogenetic banding and that the respective precision of mapping by measurement versus banding be evaluated by direct correlation. In collaborative ef-

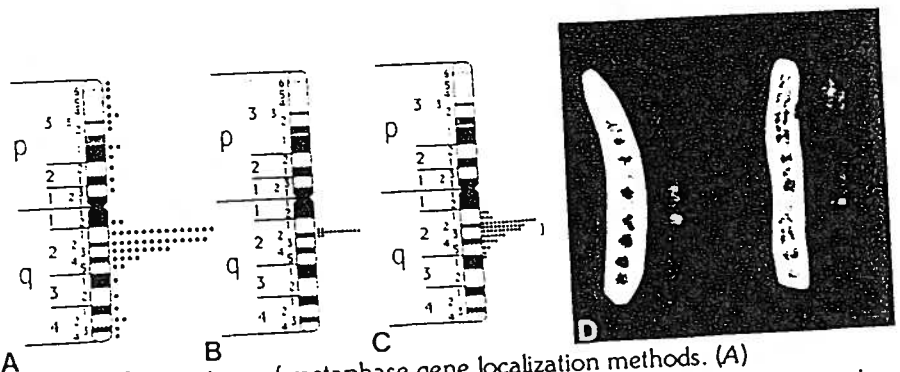

Figure 5 Comparison of metaphase gene localization methods. (*A*) Autoradiographic detection of the *Blast-1* gene on G-banded chromosomes using a ^{3}H-labeled cDNA probe. (Reprinted, with permission, from Staunton et al. 1989.) (*B*) Fluorescence detection on G-banded chromosomes. Metaphase figures were Giemsa/trypsin-banded, photographed, and then rephotographed after fluorescein-avidin detection of hybridization with *Blast-1* genomic phage probes. The total chromosome morphology was visible with fluorescein staining because of residual hybridization to repetitive DNA, allowing precise alignment on a grid of the Giemsa-stained and fluorescein-stained chromosomes, using centromeres and telomeres as reference points (see *D*). Although the prior trypsin banding treatment does weaken the hybridization signal slightly, this 20-kb target was still clearly detectable. Data points are represented with smaller dots than those in *A*, to accommodate the more precise placement of the fluorescent signals. (Reprinted, with permission, from Staunton et al. 1989.) (*C*) Fluorescent detection on unbanded chromosomes. Signals were localized by measuring along the chromosome length. To correct for differential chromosome condensation, each data point was expressed as the ratio: distance from telomere to signal/total chromosome length. (Reprinted, with permission, from Lawrence et al. 1990a, copyright AAAS.) (*D*) Trypsin G-banded chromosomes and the corresponding fluorescent signal for the *Blast-1* gene, as described in *B*.

forts, we have adapted various cytogenetic banding techniques, including G, Q, and replication, for fluorescence mapping of several human genes (Staunton et al. 1989; Takahashi et al. 1989; Brown-Shimer et al. 1990). Fluorescence mapping has also been used in conjunction with posthybridization R-banding (Viegas-Pequignot et al. 1989). A direct comparison between banding versus measurement (Fig. 5B,C) showed that fluorescence mapping on either banded or unbanded chromosomes provides improved precision over autoradiography (Fig. 5A). However, fluorescence detection coupled with banding provided the most accurate and precise placement, independent of chromosome condensation (Fig. 5B). This allowed the *Blast-1* gene to be localized near the interface of bands q21 and q22, a much smaller region than defined by the autoradiographic localization to all of q21–q23 (Staunton et al. 1989). The fluorescence detection results narrow the localization to a region encompassing approximately 5–7 Mb of DNA, or approximately 2–3% of the total chromosome length (250 Mb). The nonisotopic technique can be done in 1–2 days, whereas the autoradiography takes from weeks to

months. Restricting the measurements to highly elongated chromosomes (Fig. 5C, bar) decreases the range significantly, based on a smaller sample size. However, this approach is still somewhat less precise than the localization obtained by coupling fluorescence detection with banding. Furthermore, the range of measurements on elongated chromosomes (Fig. 5C, bar) shifted the gene position slightly to a different band on the ideogram than that identified by direct banding. We observed a similar inconsistency for the dystrophin gene, known by several criteria to map at Xp21.2 (Davies et al. 1983), but which maps just below this to Xp11.4, based on average measurements. Correlation between measurements and bands is subject to some inaccuracy because the placement of bands on the ideograms is not based strictly on measurement, since relative band position varies with condensation and other technical factors (Harnden and Klinger 1985).

Chromosome banding procedures Giemsa/trypsin banding is a method of choice for high-quality banding patterns and was the first of several banding procedures that we coupled with fluorescence gene mapping. However, Giemsa stain is highly reflective, so simultaneous visualization of bands and fluorescent signal is not possible. As illustrated in Figure 5D for localization of the *Blast-1* gene (Staunton et al., 1989), trypsin banding can be performed and photographed prior to hybridization. The slides are then rinsed in 3:1 methanol/acetic acid before hybridization to remove the Giemsa and preserve the morphology of trypsinized chromosomes. The position of each metaphase spread must be recorded and relocated for photography after hybridization, and the banded and hybridized chromosome photographs must be properly aligned to obtain an accurate placement. Although the quality of bands is not diminished by this approach, the fluorescent hybridization signals may be less intense.

Q bands can be obtained by 4,6-diamidino-2-phenylindole dihydrochloride (DAPI) staining, which fluoresces blue, distinct from the fluorescein or rhodamine generally used to detect signals. As illustrated in Figure 6, DAPI banding is extremely simple, reproducible, and does not diminish hybridization signals. Although the detail of the banding is less than that obtainable by G-banding, the contrast of the bands is improved by incorporation of 5-bromodeoxyuridine (BrdU) into late-replicating DNA. DAPI staining is done after hybridization and viewed with a separate filter, so relocation of spreads is not necessary, although alignment of the two photographs for bands and signals is.

To avoid the necessity for two photographs that must be aligned, we have worked toward developing a rapid method for simultaneous visualization of bands with hybridization signals by two-color fluorescence, using a commercially available double-label filter set. BrdU incorporation into G bands (Vogel et al. 1986) is detected by addition of a

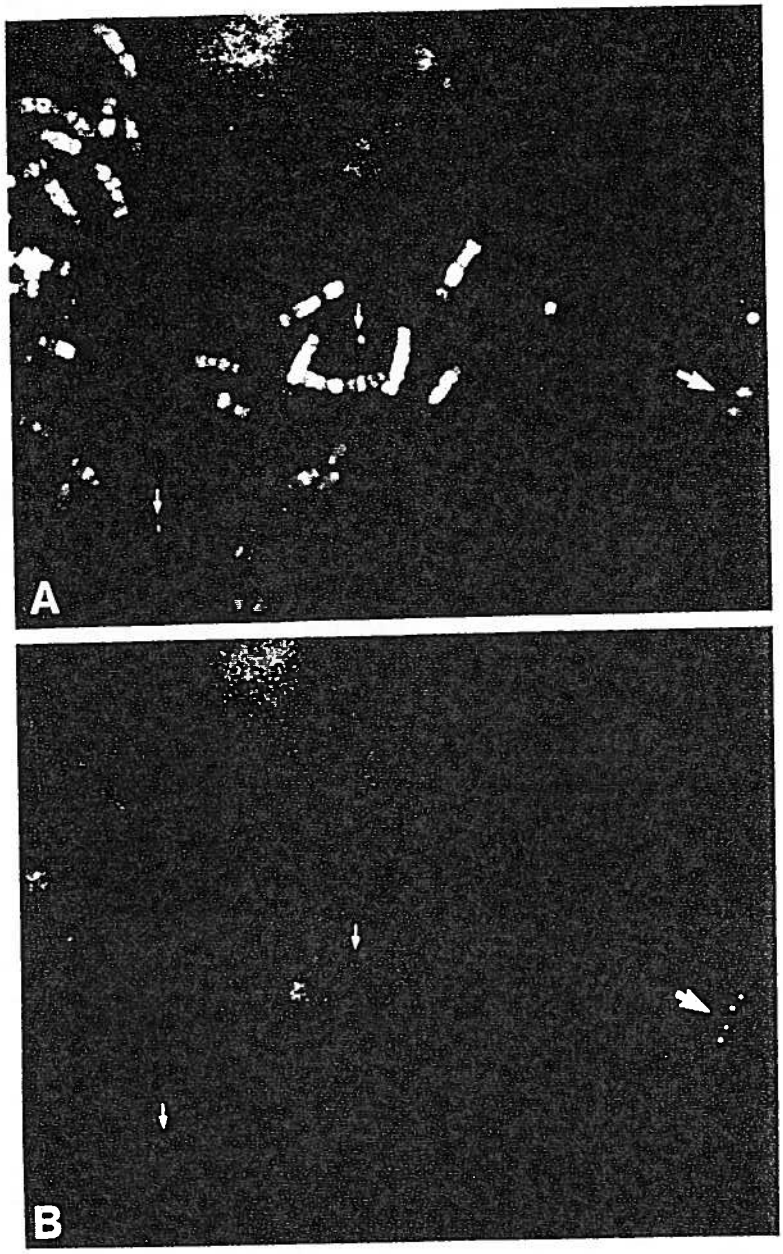

Figure 6 Localization of PTPase gene on DAPI-banded human chromosomes. (*A*) DAPI staining of chromosomes gives a Q-banding pattern, which is enhanced by incubation of cell in BrdU 7 hr prior to fixation. Arrows indicate chromosome 19, which has a morphology similar to that of chromosome 20 but is distinguishable by its Q-banding pattern. (Reprinted, with permission, from Brown-Shimer et al. 1990.) (*B*) Fluorescein-avidin detection of phage sequence of the human placental tyrosine phosphatase gene (Brown-Shimer et al. 1990) on chromosome 20.

fluoresceinated antibody to the probe-detection step, providing a rapid and convenient means of chromosome identification (see Fig. 9F). The important advantage is that bands and signals can be viewed and photographed simultaneously using a single filter set, which allows simultaneous detection of fluorescein and Texas Red. This alleviates the problems associated with superimposing or aligning separate images or the shifts that occur while making double exposures using two different filters. BrdU banding takes advantage of the fact that G bands contain primarily late-replicating DNA. Cells are grown in BrdU for a period of time that allows the cells in late S phase to progress to metaphase. Commercially available anti-BrdU antibodies require that the DNA be denatured; however, we have found that after hybridization, there is enough denatured genomic DNA to produce an excellent banding pattern. The resolution and contrast of the bands are good, although they vary in size depending on the time that individual cells spent in S phase while exposed to BrdU. Further details on this procedure are described elsewhere (McNeil et al. 1990).

Finally, hybridization to a specific repetitive element can be exploited for chromosome identification because line sequences are concentrated in the dark G bands and *Alu* sequences are concentrated in the light G bands (Manuelidis and Ward 1984; Korenberg and Rykowski 1988). This is also a convenient way to visualize signals and bands simultaneously, although the contrast and resolution of the bands are not as well defined as with other techniques.

Limits of metaphase mapping Simultaneous localization of probes along the length of unbanded chromosomes is clearly valuable for rapidly determining the relative order of sequences. A key question concerns the limit of resolution of this approach. To address whether metaphase mapping can be used in the 1-Mb range, we used the large well-characterized human dystrophin gene (Koenig et al. 1987) as a test system. This analysis (Lawrence et al. 1990a) demonstrated that sequences separated by 1.1 Mb are generally resolvable across the *width* of each chromatid, but only on more-condensed chromosomes (Fig. 7C). On longer chromosomes from less-condensed metaphase spreads, the two signals coalesced into one. Analysis of a large number of metaphases for hybridizations representing distances of 125, 375, 500, 675, and 750 kb indicated that sequences separated by a few hundred kilobases or more frequently produced barely resolvable signals on each chromatid of more contracted chromosomes but that the configuration of "doublet" signals was variable and condensation-dependent. Hence, dystrophin sequences separated by 1 Mb were not resolved along the chromosome length and could not be ordered. Even with two-color detection systems (see below), the chromosomal order of sequences separated by 750 kb was not apparent. Other observations indicate that the practical limits of

metaphase mapping may be closer to a few megabases. For example, hybridization to loosely linked *neu* and nerve growth factor receptor sequences, separated on chromosome 17 by several centiMorgans (roughly equivalent to several megabases), can be resolved and ordered along the *length* of longer chromosomes but with little separation between them (see Fig. 7B). The ability to order closely linked sequences on chromosomes is limited because the chromosome width is of sufficient dimension to encompass substantial lengths of DNA.

Interphase mapping

Metaphase mapping is important for rapid localization to a small chromosome region, but complete mapping of the human genome will largely involve analysis of sequences not far enough apart to be ordered at metaphase. Our initial work on the EBV genome, described above, indicated that higher-resolution localization within less-condensed interphase nuclei (routinely present on the same slides) provided the opportunity for mapping at a much higher resolution (Lawrence et al.

Figure 7 Results of fluorescence in situ hybridization, presented in order of decreasing physical distance. (*A*) Hybridization of a chromosome-1 sequence to cytogenetic preparations of the Namalwa cell line, illustrating how a cytogenetic abnormality is evidenced by the nonidentical labeling of sister homologs. On the basis of an estimate of 250 Mb for the DNA content of chromosome 1, the duplicated sequences are separated by 70 Mb of DNA. Note that three signals, rather than two, are observed within the interphase nucleus. The duplicated sequences from one homolog are ~5 μm apart at interphase. (*B*) Simultaneous hybridization to *neu* (*erbB2*) and nerve growth factor receptor cosmid clones, which are loosely linked and frequently resolvable along the length of less-condensed metaphase chromosomes. These sequences have been localized to separate bands (17 q11.2–q12 and 17 q21.3–q23, respectively) and are ~10 cM apart (~10 Mb) based on their respective proximity to the neurofibromatosis (NF1) locus (White et al. 1987). (*C,D*) Resolution of sequences across the width of metaphase chromosomes. After simultaneous hybridization of two probes separated by >500 kb, two discrete signals on either side of the chromatid axis are frequently observed (*C*). In contrast, hybridizations with probes separated by smaller distances generally result in one fluorescent signal on each sister chromatid (*D*), as does single-probe hybridization. The distance between paired signals on each chromatid is variable and relates to the degree of chromosome condensation. (*E*) Interphase nucleus of male PBLs showing hybridization to two sequences within the dystrophin gene separated by ~1050 kb. (*F*) Same as in *B*, except sequences are separated by 375 kb. (*G,H*) High resolution of sequences within interphase nuclei of intact, paraformaldehyde-fixed WI38 fibroblasts (derived from a female). (*G*) Dystrophin sequences separated by 650 kb are clearly separated and resolvable in ~90% of the nuclei. (*H*) Very closely paired signals are frequently (~20% in WI38) resolvable after hybridization with the α-cardiac MHC probe, which is homologous to both the α and β MHC genes on chromosome 14 (Saez et al. 1987). (*I*) Lower magnification view of hybridization to two overlapping cosmid probes for the *neu* proto-oncogene (*erbB2*). The probes produce one large signal for each chromosome-17 homolog, with no evidence of closely spaced pairs. These sequences are generally localized in the internal region of lymphocyte nuclei and hence illustrate the maximal degree of homologous pairing of any sequences tested thus far. (*C–I* reprinted, with permission, from Lawrence et al. 1990a, copyright AAAS.)

1988). It indicated that the order of sequences could be determined either (1) on the basis of the distances between probes hybridized two at a time or (2) by visualizing the interphase configuration of three or more signals simultaneously. It was important to assess whether average interphase distance correlated with linear DNA distance in the valuable 100 kb to 1 Mb range, since the folding and looping of the chromatin fiber (Paulson and Laemmli 1977; Lewin 1985) might distort this relationship at these distances. Because so little is known about higher-level chromatin packaging, it could not a priori be predicted how this relationship might vary in different cells or different areas of the genome. Trask et al. (1989) showed a correlation between interphase distance and known DNA distance up to 250 kb in the dihydrofolate reductase (*dhfr*)

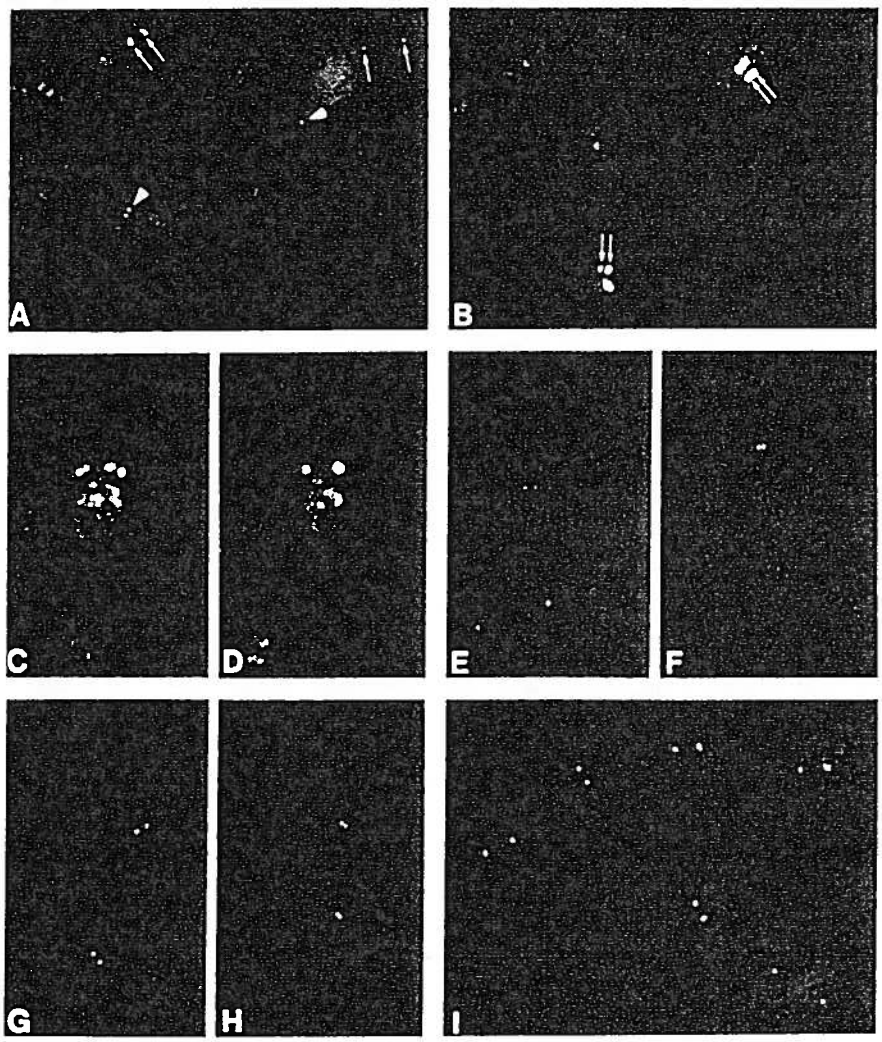

Figure 7 *(See facing page for legend.)*

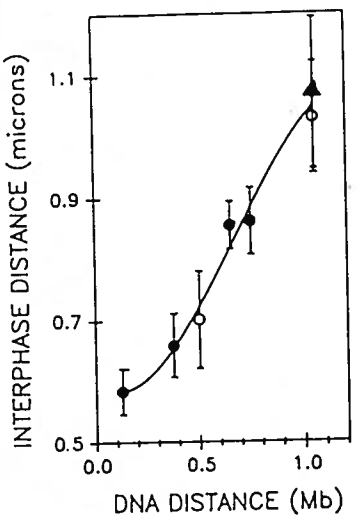

Figure 8 Relationship between DNA distance and interphase distance of dystrophin sequences. Symbols indicate the average ± S.E.M. All points were determined in normal PBLs, except that the 1-Mb distance was determined in both PBLs (*circles*) and in primary G_1-arrested WI38 fibroblasts (*triangle*). (*Closed symbols*) Data sets of 35–60 nuclei; (*open circles*) data sets of 16–20 nuclei. Distances presented in micrometers have been corrected for magnification. The curve was derived by third-order regression analysis from PBL data and is presented for emphasis. Although the relationship in this size range appears generally linear, the larger picture would predict a curve with a gradually decreasing slope, as suggested by other observations for smaller (MHC, 25–30 kb ≈ 0.1–0.2 μm) and larger distances (6 cM, ~6 kb = 2.81 μm; 70 Mb ≈ 6 μm). (Reprinted, with permission, from Lawrence et al. 1990a, copyright AAAS.)

locus of the Chinese hamster cell line. The correlation was sufficient to allow correct ordering of several cosmids in this range. To study normal human sequences up to 1 Mb apart, we analyzed dystrophin sequences within diploid human cells (Lawrence et al. 1990a). As expected for X-chromosome sequences, single-probe hybridization to male lymphocytes produced a single signal, with the exception of a small fraction of nuclei (shown to be in G_2) that contained two very closely spaced signals representing replicated DNA (Lawrence et al. 1990a). In marked contrast, targeting two sites separated by 1 Mb produced two precise, closely spaced signals in the majority of nuclei (Fig. 7C), as did hybridizations to several smaller intervals ranging from 125 to 750 kb (Fig. 7D). Hybridization with two overlapping cosmid clones (*erbB2*) produced only one hybridization signal for each of the two chromosome-17 homologs in different parts of the nucleus (Fig. 7I).

Importantly, smaller (300 and 375 kb) versus larger (675 and 750 kb) distances could be discerned by just a 5-minute examination per slide directly through the microscope. Despite a normally distributed variation from cell to cell, average interphase distances for a number of intervals showed a strong correlation with known DNA distance (Fig. 8). The overall correlation in the 1-Mb range approximated linearity, although this represents a linear region of a curve with a decreasing slope, as indicated by the observation that sequences separated by 6 cM (~6 Mb) were 2.8 μm apart, and sequences 70 Mb apart were only about 6 μm apart at interphase (see Fig. 7A). The correlation is sufficient to allow correct ordering of distances differing by 75–150 kb in the 1-Mb range (Lawrence et al. 1990a) and possibly as little as 40–50 kb for smaller distances (Trask et al. 1989). Although the relationship between interphase distance and DNA distance is not yet fully characterized and

may vary with the particular region of the genome studied, it is encouraging that the three different systems studied thus far (EBV in human lymphoma cells, *dhfr* sequences in Chinese hamster cells, and dystrophin gene sequences in normal diploid human lymphocytes) exhibited similar condensations at a given distance. As shown in Figure 8, the 1-Mb intragenic distance for dystrophin measured in two different cell types (peripheral blood lymphocytes [PBLs] and G_1-arrested WI38 fibroblasts) yielded remarkably close interphase distances.

The lower limit of interphase resolution is clearly less than 100 kb for dystrophin sequences, and several observations indicate that sequences separated by about 25 kb are just at the limit of resolution of fluorescence microscopy (0.1–0.2 μm apart). Trask et al. (1989) showed resolution of sequences separated by 25 kb for Chinese hamster chromatin. We have observed resolution of EBV sequences separated by 50 kb, and presumably as well as sequences in two highly homologous α-cardiac MHC genes spaced 25–30 kb apart (Fig. 7H). Very small distances are more approachable by gel electrophoresis; however, it is likely to prove important for ordering efforts that two sequences only 25–100 kb apart can be visually discerned from overlapping clones (Fig. 7I).

Collectively, these studies from our laboratory and others demonstrate an approach to gene mapping whereby the physical proximity of sequences, ranging from nonsyntenic to almost overlapping, can be directly assessed within intact nuclei or chromosomes. Using this cytological procedure, one can visually resolve DNA sequences one to two orders of magnitude closer than resolvable by genetic recombination analysis, autoradiographic in situ hybridization, or standard somatic cell hybridization. Estimates of actual DNA distance are approximate and should be based on an average of many nuclei because there is considerable intercell variation. However, it should be emphasized that for most applications, quantitative statistical analysis is not required because brief microscopic inspection is sufficient to distinguish between the outcomes predicted in Figure 3 and between interphase distances differing by a few hundred kilobases. The order of three probes can be easily assessed at interphase (or metaphase) using two-color detection with dual-band filters (see below). The amount of data obtained from each sample may be enhanced further by development of more complex labeling schemes; however, these may not become widely available without sophisticated imaging equipment. This potentially rapid and straightforward approach, clearly advantageous for metaphase mapping, may provide a valuable complement or alternative to other fine-structure mapping techniques, particularly PFGE. As summarized in Figure 2, the combination of interphase and metaphase fluorescence hybridization provides a needed approach for gene mapping that extends across a broad range of physical distances.

There are several types of genetic applications for which this tech-

nique may be useful. This approach could greatly facilitate the ordering of fragments from the same chromosomal region, which is often difficult or impossible by the other techniques. A combination of metaphase and interphase analysis might allow a relatively rapid means of ordering a series of overlapping cosmids or yeast artificial chromosome (YAC) clones or of screening clones for those close to a marker for a disease gene or those lying between two flanking markers for a sequence of interest. Using irradiation hybrids (Cox et al. 1989), it has recently been shown that the frequency of chromosome breakage after irradiation correlates with genomic distance. In situ hybridization could be coupled with an analysis of irradiation breakage between two or more probes directly in individual cells, obviating for many purposes the need for laborious production and characterization of numerous hybrid clones.

SPECIALIZED MICROSCOPY TECHNIQUES

Recent years have seen a dramatic increase in sophisticated equipment used for analysis of visual data, particularly for fluorescence micro-

Figure 9 (*A*) Propidium-iodide-stained chromosomes showing fluorescein detection of an 18-kb sequence of the integrated EBV genome on each sister chromatid of chromosome 1. (*B*) A localized "track" of EBV RNA, showing the nondiffuse distribution of primary transcripts within the nucleus. These tracks become especially elongated in the osmotically swollen nuclei of cytogenetic preparations, as shown here. (Reprinted, with permission, from Lawrence et al. 1989.) (*C*) Hybridization of a chromosome-17-specific centromeric repeat, which has weak homology with other centromeres, shows the distribution of several centromeres throughout the nucleus (counterstained with propidium iodide). The brightest signals indicate the positions of the chromosome-17 centromeres. Note that the relative positions of the centromeres and the nucleoli (two deeper red bodies) are easily determined using this approach. (*D*) Metaphase spread from γ-irradiated human lymphocyte culture showing chromosomes 1, 2, and 4 painted via fluorescence in situ hybridization using FITC and counterstained with propidium iodide. Chromosome 2 is translocated to another chromosome. (Figure courtesy of Joe Nathan Lucas and Marylin Boggensee of Lawrence Livermore Laboratory.) (*E*) Simultaneous visualization of hybridization signals with G bands identified by BrdU incorporation. This is a single photograph illustrating results directly as they appear through the microscope without computer enhancement or alignment. The use of two-color fluorescence allows direct visualization of the human *Blast-1* gene on banded chromosomes with a single dual-wavelength filter (Omega Corp.) One labeled chromosome 1 is in the middle of the field, and the other is in the upper right (Reprinted, with permission, from Lawrence et al. 1990a, copyright AAAS.) (*F*) "Double-label" hybridization of two single-copy chromosome-17 sequences shown in interphase nuclei and on metaphase chromosomes. Biotin- and digoxygenin-labeled probes are visualized using a dual-wavelength filter that allows rhodamine and fluorescein images to be simultaneously visualized with no optical shift in their positions. (*G*) Three chromosome-17 sequences hybridized simultaneously, two in rhodamine and one in fluorecein. Two sets of signals representing two homologous chromosomes can be seen in this interphase nucleus. One set shows an unambiguous red:red:green order, but the other has a less interpretable configuration. As the distance between sequences increases, larger numbers of cells need to be analyzed to determine the correct order.

scopy. An important very recent advance for standard fluorescence microscopy was the development of filter sets that allow the simultaneous visualization of two fluorochromes, such as Texas Red and FITC. These filter sets currently represent some compromise in the optimal conditions for each fluorochrome, so the intensity of signals may be reduced. They work well for directly detecting single genes with fluorescent bands (see Fig. 9E) or for precisely localizing multiple single genes (Fig. 9F). The physical ordering of sequences along the chromosome or chromatin fiber is greatly facilitated if different probes are distinguishable either by size, as described above, or, more definitively, by color using two different detection methods. Detection of as many as three large-tandem-repeat probes in different colors has been reported previously (Nederlof et al. 1989). As illustrated in Figure 9F,G, the order of three single-copy sequences can be determined using just two-color detection of probes

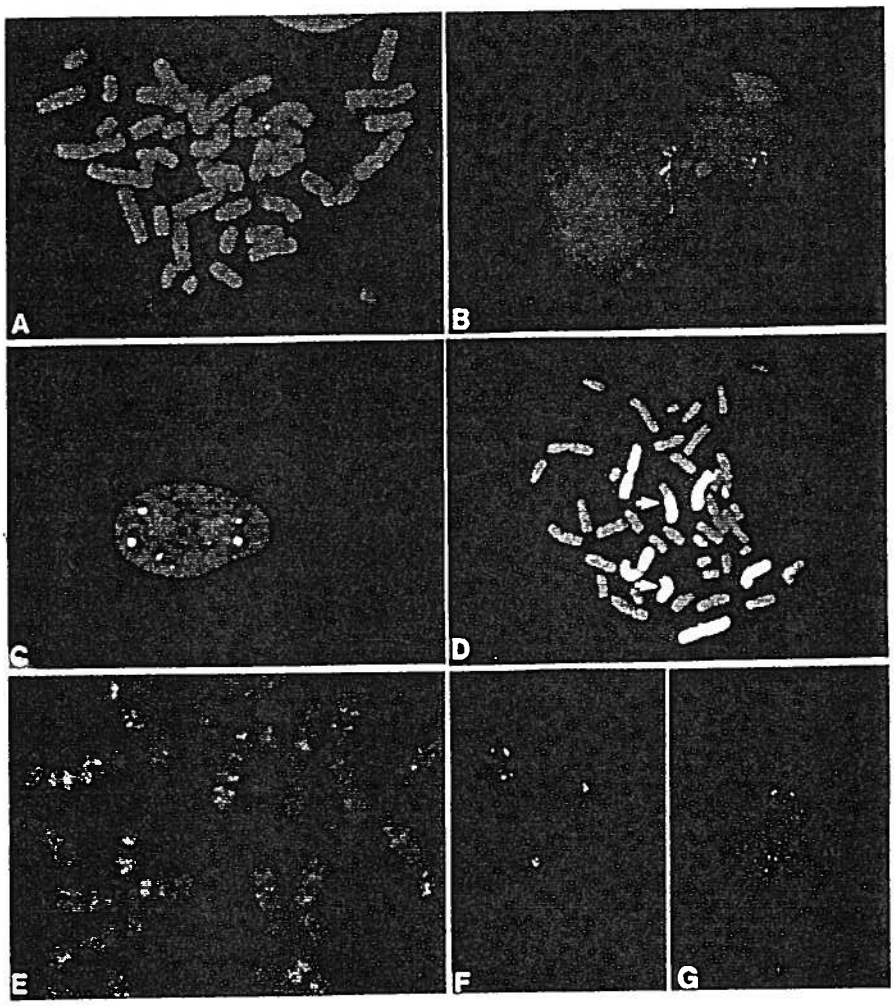

Figure 9 *(See facing page for legend.)*

labeled, for example, with biotin and with digoxygenin. High-resolution physical ordering requires extremely precise alignment of probes either by simultaneous visualization using a dual-wavelength filter set or by superimposition of separate images using sophisticated image processing. Simple double- or triple-exposure photographs, as described for multiple-color labeling of repeated sequences (Nederlof et al. 1989), are of no use in the analysis of closely spaced single-copy probes because the wavelength shift from one filter set to another is sufficient to cause a loss of precise positional information. Accurate registration of images using computer-assisted image processing is difficult and requires the use of a fiduciary marker that appears in both pictures (see Lichter et al. 1989). The development of double-label filter sets helps to avoid the equipment-intensive and often time-consuming computer-assisted analysis of multiple-label experiments and is an inexpensive advance that is becoming widely available.

The use of computer equipment provides other important advantages. For example, capturing images digitally allows them to be processed further using software designed to enhance contrast and improve the signal-to-noise ratio by averaging images to allow detection of small signals. Direct visualization of biotinylated probes below 3 kb is difficult using a one-step fluorescein-avidin detection, although, in general, brighter signals can be obtained by antibody amplification (Pinkel et al. 1986) or 2 kb or smaller sequences can be detected by digoxygenin labeling. As illustrated in Figure 10, a digital image of hard-to-see non-amplified biotin signals (2 kb) can be greatly enhanced to make the signal more obvious. Localization of sequences of less than 4 kb using an ISIT camera and computerized image registration has been reported previously (Albertson et al. 1988; Viegas-Pequignot et al. 1989). Additionally, the recent tremendous increase in technologies for storage of digital information has made it more cost-effective to archive much larger numbers of digital images. Thus, measuring the relative distances at interphase or metaphase could be done by software application directly from an image. An essential application for the study of nuclear organization is that digital images can also be used to analyze the relative position of sequences within the interphase nucleus by taking a set of serial images at different focal planes through the nucleus (optical sectioning). These images can be processed using algorithms, which remove out-of-focus light, and displayed together using software for three-dimensional viewing.

Another important development for three-dimensional analysis has been the recent advances in design and commercial availability of confocal microscopes, which optically remove out-of-focus information in the image before it is captured and stored (Brakenhoff et al. 1985). This strategy has been used to analyze the placement of various chromosomes and highly reiterated sequences in interphase nuclei, but the

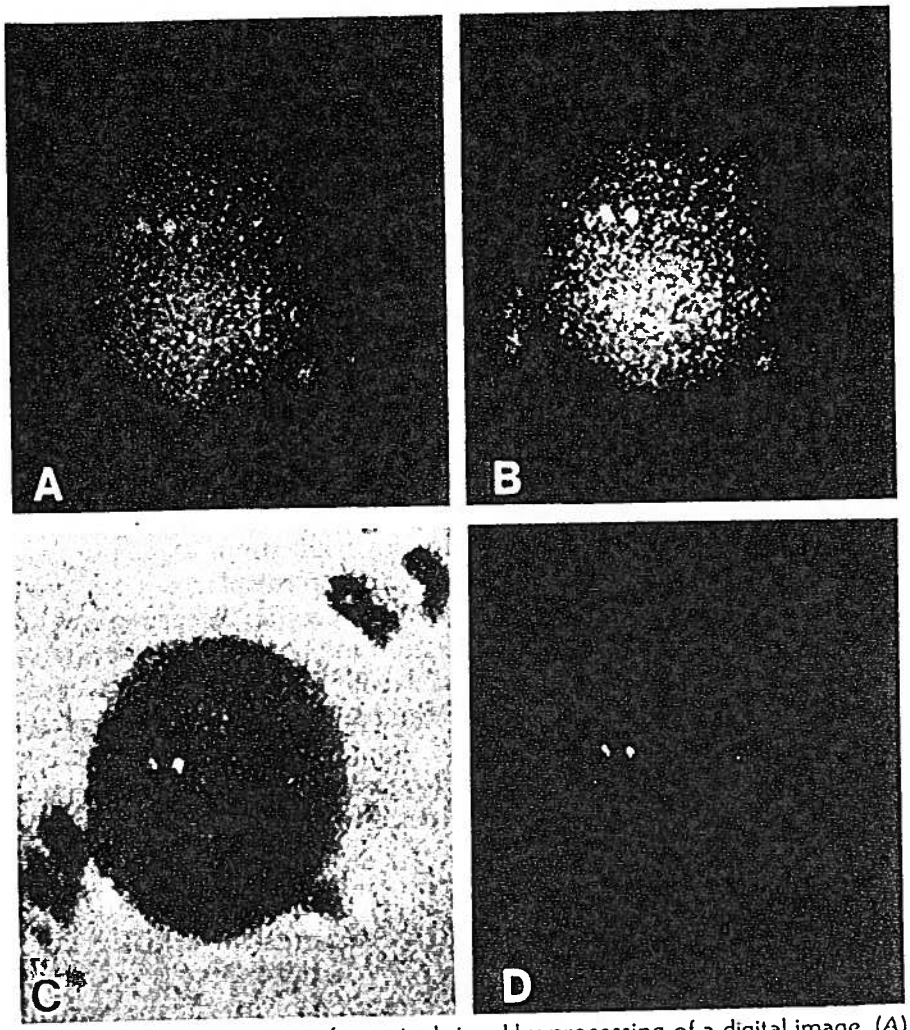

Figure 10 Improvement of marginal signal by processing of a digital image. (*A*) A 2-kb probe detected by standard fluorescence microscopy and then photographed using digital imaging microscopy. The two signals represent two copies of the EBV genome in Namalwa cell nuclei. (*B*) The same image after application of software for automatic contrast enhancement. Signals can be made even more obvious by more sophisticated processing involving the merging of images captured at different wavelengths (*C*) or the thresholding of values in the display to show only pixels with the highest intensity (*D*).

power of this approach for three-dimensional analysis of single-copy sequences has not yet been exploited.

Finally, it should be noted that the fluorescence hybridizations are amenable to quantitation and rapid analysis by techniques such as flow cytometry. Flow cytometry has been coupled with fluorescence detection of more abundant RNAs and DNAs, and this has significant potential for research and possibly diagnostic purposes. This area has been reviewed recently (Bauman et al. 1989).

POTENTIAL APPLICATIONS FOR ANALYSIS OF CYTOGENETIC ABERRATIONS

The speed, convenience, and precision of nonisotopic probe-labeling techniques make it feasible to apply cytological hybridization to the characterization of cytogenetic aberrations for both research and, potentially, diagnostic purposes. This potential has not been realized during the past decade because it is only recently that methodological capabilities have been expanded and a larger number of clinically relevant probes have become available. The current status of this technology makes possible a new area of "molecular cytogenetics," whereby standard karyotypic analysis is directly coupled with molecular biology. The field of cytogenetics has been limited to analyzing relatively gross chromosomal aberrations based on banding patterns, which includes deviations in whole chromosomes or chromosome segments containing 10 Mb or more of DNA. Using cytological hybridization, it is now possible to detect just a few kilobases of deleted or misplaced DNA anywhere within the genome. In the hunt for specific disease genes, a molecular cytogenetic defect in the gene itself might be revealed because any aberration resulting in nonidentical labeling of homologous chromosomes is readily apparent by this technique. Clearly, the technology has value for clinical research into the etiology of genetic disease, but the potential for clinical diagnostics is also strong. A few areas of potential application to cytogenetic abnormalities are summarized below.

Chromosomal aneuploidy

Hybridization of chromosome libraries, chromosome-specific centromere probes, or single-copy sequences can all make readily apparent monosomies or trisomies of specific chromosomes. The most common clinical abnormalities in this category are trisomies 21, 13, and 18 and the sex chromosome abnormalities X0, XXX, XXY, and XYY. Using a collection of several probes for the above chromosomes with multiple labels, it should be possible to screen for several aneuploidies at once. Although all of these aberrations are readily detectable by standard karyotypic analysis, an advantage of the in situ hybridization approach is that it can be done directly in interphase cells, making it unnecessary to culture cells, such as amniotic fluid cells. Cremer et al. (1986) described the use of "interphase cytogenetics" for detecting trisomy 18, and other investigators have used this approach, for example, for demonstration of trisomy 21 (Lichter et al. 1988; Pinkel et al. 1988).

Translocations

Chromosome libraries or specific repeats can also be used for the detection and characterization of translocations, as shown in Figure 9D. This

strategy is applicable to the detection of specific translocations known to characterize particular types of cancers. In addition, translocations that appear to be balanced can be analyzed much more precisely using a battery of probes for a specific chromosomal region. Translocations may be even more readily detected at interphase using two probes known to flank the breakpoint, which will be detected unusually close together (on the same chromosome) when the translocation is present. We are currently using two-color hybridization to screen for probes between flanking sequences.

Deletions

Submicroscopic deletions involving a few kilobases or more of DNA are readily apparent by in situ hybridization. There are many areas in which this might be useful, for example, in carrier detection. Heterozygous gene deletions are difficult to identify by Southern blot analysis because heterozygosity is manifest only as the change in intensity of a band, which is often difficult to discern. In contrast, with in situ hybridization, heterozygosity is readily apparent as the total absence of signal on one homolog. (The presence of signal on the other homolog serves as an internal positive control.) Because hybridization efficiency is high (>90%), deletions can be confidently identified by analysis of just a few cells. An example of how in situ deletion detection might be useful is provided by Duchenne's muscular dystrophy, for which the most common molecular defect has been identified as deletions of 6 kb or more in the dystrophin gene (Koenig et al. 1987). Once a specific deletion is identified in an affected male by filter hybridization with different probes, female family members can easily be screened for the same deletion using metaphase or interphase analysis (J.B. Lawrence and J.A. McNeil, in prep.) Affected individuals themselves might be screened with a small battery of probes for the most common deletions. As specific defects in inherited diseases or\cancer are identified and characterized, the number of potential applications will grow. This application may prove to be very important in the diagnosis of tumor suppressor gene deletions in interphase cells.

NUCLEAR ORGANIZATION

Efforts to describe and completely understand the organization of complex genomes will ultimately include investigations into the three-dimensional organization of these genes in their functional state at interphase. The nuclear genome is not simply a linear structure; hence, it is important not only to provide a detailed linear map and sequence, but also to seek concomitantly the basic principles and functional significance of its total in vivo organization. High-resolution in situ hy-

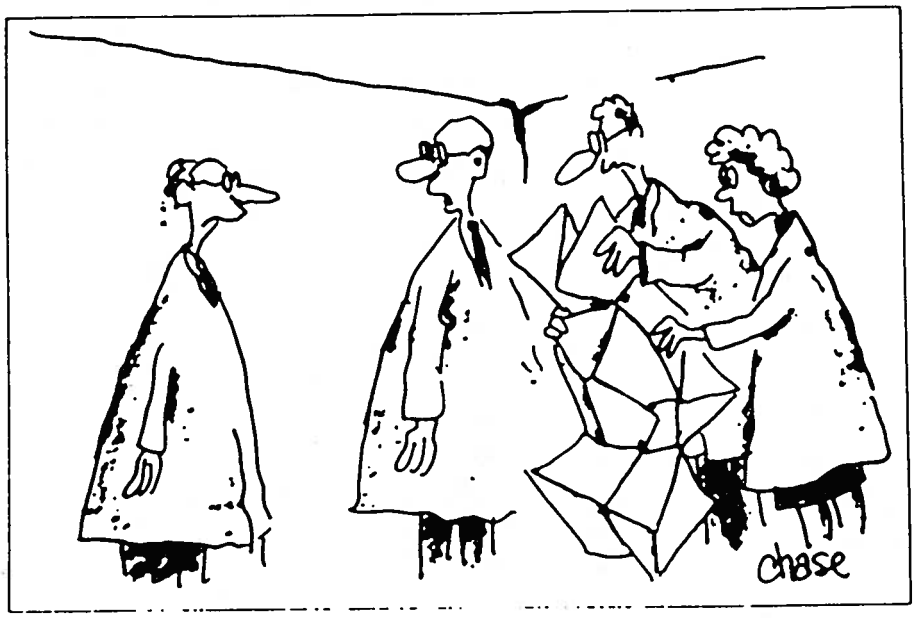

"We finished the genome map, now we can't figure out how to fold it!"

bridization provides a powerful approach for investigation of higher-level chromatin packaging, localization of specific genes within the nucleus, potential changes in nuclear organization with different functional states, and the processing and transport of nuclear RNAs.

Efforts to understand the relationship between gene organization and gene function may be most appropriately applied to chromatin in its functional state, at interphase. In recent years, much has been learned about the nucleosome structure of chromatin (for review, see Hamkalo and Rattner 1980; Georgiev et al. 1981; Weisbrod 1982), but, as mentioned above, little is known about the higher-level organization. Since first proposed (Rabl 1985), an order to the three-dimensional distribution of chromatin in the interphase nucleus has been suggested by a variety of cytological observations (Comings 1968, 1980; Cremer et al. 1982; Agard and Sedat 1983; Manuelidis 1984, 1985; Schardin et al. 1985; Hochstrasser et al. 1986; Hochstrasser and Sedat 1987), and it has been suggested that active genes are localized in specific nuclear domains (Hutchinson and Weintraub 1985). However, the detailed investigation of nuclear organization is at an early stage and has been restricted primarily to repetitive sequences or nuclear landmarks, such as the nucleolus. Much more refined analysis can now be done because the tools are now available for localization of specific single-copy genes within nuclei. This type of analysis showed, for example, that the EBV genome was confined to the inner 50% sphere of the nucleus, strongly indicating a sequence-specific higher-level order within interphase chromatin (Lawrence et al. 1988).

Fluorescence hybridization at interphase or metaphase can also provide important information about intermediate folding or "packaging" of chromatin. DNA is complexed with histones into a 300-Å fiber, which provides a packaging ratio of 25–40:1 (Weisbrod 1982; Lewin 1985), and although higher-level looping seems to occur (for review, see Hamkalo and Rattner 1980; Lewin 1985), exactly how the 300-Å fiber is folded into chromatin and chromosomes is unknown. Direct measurements of physical distance at interphase between closely spaced genes has not been studied because of the unavailability of sensitive, sequence-specific detection methods. This type of investigation can now be done using nonisotopic in situ hybridization. Direct measurement of distances within the dystrophin gene resulted in several observations that provide important clues about chromatin packaging and nuclear organization (Lawrence et al. 1990a).

1. Initially, it was shown that the unexpected resolution between closely spaced sequences was not primarily a consequence of the cytogenetic spreading methodology, since a comparable degree of resolution was observed after hybridizations to intact monolayer fibroblasts preserved with paraformaldehyde.
2. Two different normal cell types, PBLs and primary fibroblasts, have a remarkably similar condensation despite gross differences in nuclear size and morphology (Table 2). This suggests that for lengths of DNA up to 1 Mb, a fundamental level of chromatin packaging is measured that is common to nuclei with different gross nuclear organizations.
3. Similar to previous measurements of condensation for integrated viral DNA in human cells (Lawrence et al. 1988) and hamster DNA (Trask et al. 1989), the condensation for a normal human gene at the 125-kb distance is approximately 1:73, close to the 1/40–1/50 packaging ratio (PR) predicted for the 30-nm chromatin fiber (Lewin 1985). It must be considered that the hybridization process may affect chromatin condensation; however, these results are not inconsistent with estimates

Table 2 Changes in DNA condensation with increasing length

DNA distance (kb)	Packaging ratio
125	1:73
375	1:194
500	1:242
675	1:296
1050	1:334
1050 (WI38)	1:347

of overall condensation at interphase of 10^3 or more (Lewin 1985), because the distance between very close sequences is less affected by higher-level chromatin folding. The PR increases with DNA distance up to 1:334 at 1 Mb (Table 2). For sequences separated by approximately 70 Mb on chromosome 1 (see Fig. 7A), the PR increases dramatically to 1:2000–1:3000. Since condensation at 1 Mb is still quite small, the repeating unit of chromatin organization that establishes the greater PR must involve significantly longer stretches of DNA.

4. In metaphase chromosomes, sequences just 1 Mb apart are frequently separated across the chromatid width, suggesting that the chromatin fiber may cross the chromatid axis in relatively short stretches of DNA (see Fig. 7C).
5. Replicated "sister-chromatin" genes are closely aligned within S/G_2 interphase nuclei (see Lawrence et al. 1990a). Consideration of this is essential for interphase mapping and also demonstrates an approach for precise timing of specific gene replication within single cells.
6. Finally, for four different individual genes, the homologous sequences are not somatically paired within lymphocytes or fibroblasts (see Fig. 7).

An additional feature of this methodology, which has already provided important insights into nuclear structure and has the potential to contribute to investigations of genetic disease, is the ability to detect primary nuclear transcripts from expressed genes. High-resolution visualization of specific viral RNAs has revealed very localized, often curvilinear, "tracks" of nuclear RNAs (see Fig. 9B) (Lawrence et al. 1989). This strongly suggests a highly structured nuclear interior in which RNA is not freely diffusing, and recent experiments suggest that this RNA may be tightly associated with a nonchromatin fibrillar matrix (Y. Xing and J.B. Lawrence, in prep.). Detailed study of nuclear RNA in concert with DNA localization will provide important clues to the overall organization and function of the genome. Other possible applications for nuclear RNA detection are for investigating genetic disease or for screening cloned genomic DNA sequences to find those that are expressed. Aberrant gene expression can result from a defect at one of several steps from gene to active protein. In Duchenne's muscular dystrophy, a significant fraction of genetic defects in the dystrophin gene (other than the 50% known to be deletions) may result from defects in the enormous degree of processing that the dystrophin transcripts must undergo. Nonisotopic in situ hybridization provides a potential tool for detecting defects in RNA processing that may result in accumulated nuclear RNA. If defective RNA does accumulate, it may also reveal information about where in the nucleus certain RNA processing steps occur.

BRIEF HYBRIDIZATION PROTOCOL

Normal human PBLs are prepared by standard techniques from PBLs using hypotonic treatments in 0.75 M KCl and fixation in 3:1 methanol:acetic acid. Where needed, BrdU is added to the culture 7 hours before harvesting. Slides are air-dried overnight and then stored at –80°C.

Probes are nick-translated with biotin-16 dUTP or digoxygenin-11 dUTP (Boehringer Mannheim) by standard methodology. DNase I concentration is carefully monitored to provide fragments an average of 200–400 bp in length, taking care that the full range does not extend beyond 700 bp. After nick translation, 20 µg each of sonicated salmon sperm and *Escherichia coli* tRNA are added for every microgram of probe. Probes are ethanol-precipitated to remove free nucleotides and salt. The pellet is resuspended in water and stored at 4°C.

For each slide, 50–100 ng of each probe plus 0.5–100 µg of competitor (if required) are lyophilized in an microcentifuge tube. Slides of cytogenetic preparations are baked at 65°C for 1–3 hours prior to denaturation to harden and preserve morphology. For detection of DNA, the slides are denatured in 70% formamide, 2× SSC, at 70°C for 2 minutes and then immersed in 70% ethanol until all of the slides are denatured. They should then be dehydrated through 95% and 100% ethanol and air-dried. Lyophilized probe is resuspended in 10 µl of 100% formamide and denatured at 75°C for 10 minutes. Hybridization buffer (10 µl) (2 parts 50% dextran sulfate, 1 part 10 mg/ml bovine serum albumin [BSA], 1 part 20× SSC, and 1 part double-distilled deionized H_2O) is mixed into each tube, and the probe is then applied to the slide.

Hybridization is performed at 37°C for a minimum of 3 hours to overnight. Samples are rinsed for 30 minutes each in 50% formamide, 2× SSC at 37°C; 2× SSC at 37°C; and 1× SSC at room temperature. Slides are stained with fluorescein-avidin (10 µg/µl in 4× SSC, 1% BSA) for 30–60 minutes at 37°C and rinsed in 4× SSC, 4× SSC/0.05% Triton, and 4× SSC for 10 minutes each. Anti-BrdU (Becton Dickinson; Boehringer Mannheim 1:1000) and/or antidigoxygenin (1:200; Boehringer Mannheim) can be applied simultaneously with the fluorescein-avidin. Depending on the color of the fluorescent label, a counterstain may be desired using either DAPI or propidium iodide. Samples are mounted in antibleach media (90% glycerol, 1× PBS, and 2.5% di-amidino-bi-cyclo-octane (DABCO); Sigma) and viewed with epifluorescence optics.

Acknowledgments

The work from our laboratory summarized here resulted from the collective effort of several people. In particular, much of this work was done in collaboration with Dr. Robert Singer. Carol Villnave Johnson has been a strong contributor to the development of the basic technol-

ogy for several years, and John McNeil has been primarily responsible for developments in human gene mapping. In addition, the assistance of Ken Carter in the preparation of the manuscript and conceptualization of Figure 2 is appreciated, as is the contribution of Lisa Marselle to the work on primary transcript detection of EBV and HIV. Assistance in photographic processing and manuscript preparation were provided by Marie Picard-Craig, Mike Gerdes, Cindy Beaudry, and Lauric Sullivan.

References

Agard, D. and J. Sedat. 1983. Three-dimensional architecture of a polytene nucleus. *Nature* 302: 76.

Albertson, D.G. 1985. Mapping muscle genes by in situ hybridization using biotin-labeled probes. *EMBO J.* 4: 2493.

Albertson, D.G., R. Fishpool, P. Sherrington, E. Nacheva, and C. Milstein. 1988. Sen-sitive and high resolution in situ hybridization to human chromosomes using biotin labelled probes: Assignment of the human thymocyte CD 1 antigen genes to chromosome 1. *EMBO J.* 7: 2801.

Bauman, J., D. Pinkel, B. Trask, and M. van der Ploeg. 1989. Flow cytometric measurement of specific DNA and RNA sequences. In *Flow cytogenetics* (ed. J.W. Gray), p. 275. Academic Press, New York.

Bauman, J.G.J., J. Wiegant, P. Borst, and P. van Duijn. 1980. A new method for fluorescence microscopical localization of specific DNA sequences by in situ hybridization of fluorochrome-labelled RNA. *Exp. Cell Res.* 128: 485.

Bauman, J.G.J., J. Wiegant, P. van Duijn, N.H. Lubsen, P.J.A. Sondermeijer, W. Hennig, and E. Kubli. 1981. Rapid and high resolution detection of in situ hybridization to polytene chromosomes using fluorochrome-labeled RNA. *Chromosoma* 84: 1.

Botstein, D., R.L. White, M. Skolnick, and R.W. Davis. 1980. Construction of a genetic linkage map in man using restriction fragment length polymorphisms. *Am. J. Hum. Genet.* 32: 314.

Brakenhoff, G.J., H.M.T. van der Voort, E.A. van Spronsen, W.A.M. Linnemans, and N. Nanninga. 1985. Three-dimensional chromatin distribution in neuroblastoma nuclei shown by confocal scanning laser microscopy. *Nature* 317: 748.

Broker, T.R., L.M. Angerer, P.H. Yen, N.D. Hershey, and N. Davidson. 1978. Electron microscopic visualization of tRNA genes with ferritin-avidin:biotin labels. *Nucleic Acids Res.* 5: 363.

Brown-Shimer, S., K.A. Johnson, J.B. Lawrence, C. Johnson, A. Bruskin, N.R. Green, and D.E. Hill. 1990. Molecular cloning and chromosome mapping of the human gene encoding protein phosphotyrosyl phosphatase 1B. *Proc. Natl. Acad. Sci.* 87: 5148.

Cantor, C.R., C.L. Smith, and M.K. Mathew. 1988. Pulsed-field gel electrophoresis of very large DNA molecules. *Annu. Rev. Biophys. Biophys. Chem.* 17: 287.

Comings, D. 1968. The rationale for an ordered arrangement of chromatin in the interphase nucleus. *Am. J. Hum. Genet.* 20: 440.

———. 1980. Arrangement of chromatin in the nucleus. *Hum. Genet.* 53: 131.

Cox, D.R., C.A. Pritchard, E. Uglum, D. Casher, J. Kobori, and R.M. Myers. 1989.

Segregation of the Huntington disease region of human chromosome 4 in a somatic cell hybrid. *Genomics* 4: 397.

Cremer, T., C. Cremer, T. Schneider, H. Baumann, L. Hens, and M. Kirsch-Volders. 1982. Analysis of chromosome positions in the interphase nucleus of Chinese hamster cells by laser-UV-microirradiation experiments. *Hum. Genet.* 62: 201.

Cremer, T., J.E. Landegent, H. Bruckner, H.P. Scholl, M. Schardin, H.D. Hager, P. Devilee, P.L. Pearson, and M. van der Ploeg. 1986. Detection of chromosome aberrations in the human interphase nucleus by visualization of specific target DNAs with radioactive and non-radioactive in situ hybridization techniques: Diagnosis of trisomy 18 with probe L1.84. *Hum. Genet.* 74: 346.

Dale, R.M.K., E. Martin, D.C. Livingstone, and D.C. Ward. 1975. Direct covalent mercuration of nucleotides and polynucleotides. *Biochemistry* 14: 2447.

Davies, K.E., P.L. Pearson, P.S. Harper, J.M. Murray, T. O'Brien, M. Sarfarazzi, and R. Williamson. 1983. Linkage analysis of two cloned DNA sequences flanking the Duchenne muscular dystrophy locus on the short arm of the human X chromosome. *Nucleic Acids Res.* 11: 2303.

Evans, H., R. Buckland, and M.L. Pardue. 1974. Location of the genes coding for 18S and 28S ribosomal RNA in the human genome. *Chromosoma* 48: 405.

Gall, J.G. and M.L. Pardue. 1969. Formation and detection of RNA-DNA hybrid molecules in cytological preparations. *Proc. Natl. Acad. Sci.* 63: 378.

Garson, J.A., J.A. van den Berghe, and J.T. Kemshead. 1987. Novel nonisotopic in situ hybridization technique detects small (1 kb) unique sequences in routinely G-banded human chromosomes: Fine mapping of N-*myc* and β-*NGF* genes. *Nucleic Acids Res.* 15: 4761.

Georgiev, G.P., V.V. Bakayev, S.A. Nedospasov, S.V. Razin, and V.L. Mantieve. 1981. Studies on structure and function of chromatin. *Mol. Cell. Biochem.* 40: 29.

Gerhard, D.S., E.S. Kawasaki, F. Carter Bancroft, and P. Szabo. 1981. Localization of a unique gene by direct hybridization in situ. *Proc. Natl. Acad. Sci.* 78: 3755.

Hamkalo, B.A. and J.B. Rattner. 1980. Folding up genes and chromosomes. *Q. Rev. Biol.* 55: 409.

Harnden, D.C. and H.P. Klinger, eds. 1985. *An international system for human cytogenetic nomenclature*, p. 48. Karger, Basel.

Harper, M.E. and L.M. Marselle. 1985. In situ hybridization: Application to gene localization and RNA detection. *Can. Genet. Cytogenet.* 19: 73.

Harper, M.E., A. Ullrich, and G.R. Saunders. 1981. Localization of the human insulin gene to the distal end of the short arm of chromosome 11. *Proc. Natl. Acad. Sci.* 78: 4458.

Hochstrasser, M. and J.M. Sedat. 1987. Three-dimensional organization of *Drosophila melanogaster* interphase nuclei. I. Tissue-specific aspects of polytene nuclear architecture. *J. Cell Biol.* 104: 1455.

Hochstrasser, M., D. Mathoy, Y. Gruenbaum, H. Saumweber, and J.W. Sedat. 1986. Spatial organization of chromosomes in the salivary gland nuclei of *Drosophila melanogaster*. *J. Cell Biol.* 102: 112.

Hopman, A.H., J. Wiegant, G.I. Tesser, and P. van Duijn. 1986. A nonradioactive method based on mercurated nucleic acid probes and sulfhydryl-hapten ligands. *Nucleic Acids Res.* 14: 6471.

Hutchinson, N. and H. Weintraub. 1985. Localization of DNAse I-sensitive sequences to specific regions of interphase nuclei. *Cell* 43: 471.

John, H., M.L. Birnstiel, and K.N. Jones. 1969. RNA-DNA hybrids at the cytological level. *Nature* 223: 582.

Koenig, M., E.P. Hoffman, C.J. Bertelsom, A.P. Monaco, C. Feener, and L.M. Kunkel. 1987. Complete cloning of the Duchenne muscular dystrophy (DMD) cDNA and preliminary genomic organization of the DMD gene in normal and affected individuals. *Cell* 50: 509.

Korenberg, J.R. and M.C. Rykowski. 1988. Human genome organization: Alu lines and the molecular structure of metaphase chromosome bands. *Cell* 53: 391.

Kress, H., E. Meyerowitz, and N. Davidson. 1985. High resolution mapping of in situ hybridized biotinylated DNA to surface-spread *Drosophila* polytene chromosomes. *Chromosoma* 93: 113.

Landegent, J.E., N. Jansen in de Wal, R.H. Dirks, F. Baas, M. van der Ploeg. 1987. Use of whole cosmid cloned genomic sequences for chromosomal localization by non-radioactive in situ hybridization. *Hum. Genet.* 77: 366.

Landegent, J.E., N. Jansen in de Wal, G.-J.B. van Ommen, F. Baas, J.J.M. de Vijlder, P. van Duijn, and M. van der Ploeg. 1985. Chromosomal localization of a unique gene by nonautoradiographic in situ hybridization. *Nature* 317: 175.

Langer, P.R., A.A. Waldrop, and D.C. Ward. 1981. Enzymatic synthesis of biotin-labeled polynucleotides: Novel nucleic acid affinity probes. *Proc. Natl. Acad. Sci.* 78: 6633.

Langer-Safer, P.R., M. Levine, and D.C. Ward. 1982. Immunological method for mapping genes on *Drosophila* polytene chromosomes. *Proc. Natl. Acad. Sci.* 79: 4381.

Lawrence, J.B. and R.H. Singer. 1985. Quantitative analysis of in situ hybridization methods for the detection of actin gene expression. *Nucleic Acids Res.* 13: 1777.

Lawrence, J.B., R.H. Singer, and L.M. Marselle. 1989. Highly localized tracks of specific transcripts within interphase nuclei visualized by in situ hybridization. *Cell* 57: 493.

Lawrence, J.B., R.H. Singer, and J.A. McNeil. 1990a. Interphase and metaphase resolution of different distances within the human dystrophin gene. *Science* 249: 928.

Lawrence, J.B., C.A. Villnave, and R.H. Singer. 1988. Sensitive, high-resolution chromatin and chromosome mapping in situ: Presence and orientation of two closely integrated copies of EBV in a lymphoma cell line. *Cell* 52: 51.

Lawrence, J.B., L.M. Marselle, K.S. Byron, J.L. Sullivan, and R.H. Singer. 1990b. Subcellular localization of low abundant HIV nucleic acid sequences visualized by fluorescence in situ hybridization. *Proc. Natl. Acad. Sci.* 87: 5420.

Lewin, B., ed. 1985. Chromatin structure: The nucleosome. In *Genes II*, p. 469. Wiley, New York.

Lichter, P, T. Cremer, C.-J.C. Tang, P.C. Hatkins, L. Manuelidis, and D.C. Ward. 1988. Rapid detection of human chromosome 21 aberrations by in situ hybridization. *Proc. Natl. Acad. Sci.* 85: 9664.

Lichter; P., C.C. Tang, K. Call, G. Hermanson, G. Evans, D. Housman, and D.C. Ward. 1990. High-resolution mapping of human chromosome II by in situ

hybridization with cosmid clones. *Science* 247: 64.

Manning, J.E., N.D. Hershey, T.R. Broker, M. Pellegrini, H.K. Mitchell, and N. Davidson. 1975. A new method of *in situ* hybridization. *Chromosoma* 53: 107.

Manuelidis, L. 1984. Different central nervous system cell types display distinct and nonrandom arrangements of satellite DNA sequences. *Proc. Natl. Acad. Sci.* 81: 3123.

———. 1985. Individual interphase chromosome domains revealed by in situ hybridization. *Hum. Genet.* 71: 288.

Manuelidis, L. and D.C. Ward. 1984. Chromosomal and nuclear distribution of the FHind III 1.9-kb human DNA repeat-segment. *Chromosoma* 91: 28.

Manuelidis, L., P.R. Langer-Safer, and D.C. Ward. 1982. High-resolution mapping of satellite DNA using biotin-labeled DNA probes. *J. Cell Biol.* 95: 619.

Matsuo, T., M. Heller, L. Petti, E. O'Shiro, and E. Kieff. 1984. Persistence of the Epstein-Barr virus genome integrated into human lymphocyte DNA. *Science* 226: 1322.

McNeil, J.A., C.V. Johnson, K.C. Carter, R.H. Singer, and J.B. Lawrence. 1990. Localizing DNA and RNA within nuclei and chromosomes. *Genet. Anal. Tech. Appl.* (in press).

Nederlof, P.M., D. Robinson, R. Abuknesha, J. Weigant, A.H.N. Hopman, H.J. Tanke, and A.K. Raap. 1989. Three color fluorescence in situ hybridization for the simultaneous detection of multiple nucleic acid sequences in interphase nuclei and chromosomes. *Cytometry* 10: 20.

Paulson, J.R. and U.K. Laemmli. 1977. The structure of histone-depleted metaphase chromosomes. *Cell* 12: 817.

Pinkel, D., T. Straume, and J.W. Gray. 1986. Cytogenetic analysis using quantitative, high-sensitivity, fluorescence hybridization. *Proc. Natl. Acad. Sci.* 83: 2934.

Pinkel, D., J. Landegent, C. Collins, J. Fuscoe, R. Seagraves, J. Lucas, and J. Gray. 1988. Fluorescence in situ hybridization with human chromosome-specific libraries: Detection of trisomy 21 and translocations of chromosome 4. *Proc. Natl. Acad. Sci.* 85: 9138.

Rabl, C. 1885. Uber zelltheilung. *Morphologisches Jahrbuch* 10: 214.

Renz, M. and C. Kurz. 1984. A colorimetric method for DNA hybridization. *Nucleic Acids Res.* 12: 3435.

Ruddle, F.H. 1973. Linkage analysis in man by somatic cell genetics. *Nature* 242: 165.

Ruddle, F.H. and R.P. Creagan. 1975. Parasexual approaches to the genetics of man. *Annu. Rev. Genet.* 9: 407.

Rudkin, G.T. and B.D. Stollar. 1977. High resolution detection of DNA/RNA hybrids in situ by indirect immunofluorescence. *Nature* 265: 472.

Saez, L.J., K.M. Gianola, E.N. McNally, R. Feghali, R. Eddy, T.B. Shows, and L.A. Leinwand. 1987. Human cardiac heavy chain genes and their linkage in the genome. *Nucleic Acids Res.* 15: 5443.

Schardin, M., T. Cremer, H.D. Hager, and M. Lang. 1985. Specific staining of human chromosomes in Chinese hamster x human hybrid cell lines demonstrates interphase chromosome territories. *Hum. Genet.* 71: 281.

Schwartz, D.C. and C.R. Cantor. 1984. Separation of yeast chromosome-sized DNAs by pulsed field gradient gel electrophoresis. *Cell* 37: 67

Singer, R.H. and D.C. Ward. 1982. Actin gene expression visualized in chicken

muscle tissue culture by using in situ hybridization with a biotinated nucleotide analog. *Proc. Natl. Acad. Sci.* 79: 7331.

Singer, R.H., G.L. Langevin, and J.B. Lawrence. 1989. Ultrastructural visualization of cytoskeletal mRNAs and their associated proteins using double-label in situ hybridization. *J. Cell Biol.* 108: 2343.

Singer, R.H., J.B. Lawrence and R.N. Rashtchian. 1987. Toward a rapid and sensitive in situ hybridization methodology using isotopic and non-isotopic probes. In *In situ hybridization: Application to the central nervous system* (ed. K. Valentino et al.), p. 71. Oxford University Press, New York.

Singer, R.H., J.B. Lawrence, and C. Villnave. 1986. Optimization of in situ hybridization using isotopic and non-isotopic detection methods. *Biotechniques* 4: 230.

Staunton, D.E., R.C. Fisher, M.M. LeBeau, J.B. Lawrence, D.E. Barton, U. Francke, M. Dustin, and D.A. Thorle-Lawson. 1989. Blast-1 possesses a glycosyl-phosphatidyl-inositol (GPI) membrane anchor, is related to LFA-3 and OX-45, and maps to chromosome 1q21-23. *J. Exp. Med.* 169: 1087.

Takahashi, E., T. Hori, J.B. Lawrence, J. McNeil, R.H. Singer, P. O'Connell, M. Leppert, and A. White. 1989. Human type II collagen gene (COL2A1) assigned to chromosome 12q13.1-q13.2 by in situ hybridization DNA probe. *Jpn. J. Human Genet.* 34: 307.

Tchen, P., R.P.P. Fuchs, E. Sage, and M. Leng. 1984. Chemically modified nucleic acids as immunodetectable probes in hybridization experiments. *Proc. Natl. Acad. Sci.* 81: 3466.

Trask, B., D. Pinkel, and G. van den Engh. 1989. The proximity of DNA sequences in interphase cell nuclei is correlated to genomic distance and permits ordering of cosmids spanning 250 kilobase pairs. *Genomics* 5: 710.

van Prooijen-Knegt, A.C., J.F.M. van Hock, J.G.J. Bauman, P. van Duijn, I.G. Wool, and M. van der Ploeg. 1982. In situ hybridization of DNA sequences in human metaphase chromosomes visualized by an indirect fluorescent immunocytochemical procedure. *Exp. Cell Res.* 141: 397.

Verdlov, E., G.S. Monastyrskaya, L.I. Guskova, T.L. Levitan, V.I. Sheichenko, and E. Budowsky. 1974. Modification of cytidine residues with a bisulfite-O-methylhydroxylamine mixture. *Biochim. Biophys. Acta* 340: 153.

Viegas-Pequignot, E., B. Dutrillaux, H. Magdelenat, and M. Coppey-Moisan. 1989. Mapping of single-copy DNA sequences on human chromosomes by in situ hybridization with biotinylated probes. Enhancement of detection sensitivity by intensified-fluorescence digital-imaging microscopy. *Proc. Natl. Acad. Sci.* 86: 582.

Vogel, W., M. Autenreith, and G. Speit. 1986. Detection of bromodeoxyuridine incorporation in mammalian chromosomes by a bromodeoxyuridine antibody. I. Demonstration of replication patterns. *Hum. Genet.* 72: 129.

Weisbrod, S. 1982. Active chromatin. *Nature* 297: 289.

White, R., Y. Nakamura, P. O'Connell, M. Leppert, J. Lalouel, D. Barker, D. Goldgar, M. Skolnick, J. Carey, C. Wallis, C. Sluter, C. Mathew, and B. Ponder. 1987. Markers for the neurofibromatosis type 1 gene. *Genomics* 1: 364.

Wu, W. and N. Davidson. 1981. Transmission electron microscopic method for gene mapping on polytene chromosomes by in situ hybridization. *Proc. Natl. Acad. Sci.* 78: 7059.